ARTICLES
https://doi.org/10.1038/s41564-018-0182-y
nature microbiology

Chlamydia trachomatis paralyses neutrophils to evade the host innate immune response

Karthika Rajeeve[1], Sudip Das[1,2], Bhupesh K. Prusty[1] and Thomas Rudel[1]*

***Chlamydia trachomatis*, an obligate intracellular human pathogen, is a major cause of sexually transmitted diseases. Infections often occur without symptoms, a feature that has been attributed to the ability of the pathogen to evade the host immune response. We show here that *C. trachomatis* paralyses the host immune system by preventing the activation of polymorphic nuclear leukocytes (PMNs). PMNs infected with *Chlamydia* fail to produce neutrophil extracellular traps and the bacteria are able to survive in PMNs for extended periods of time. We have identified the secreted chlamydial protease-like activating factor (CPAF) as an effector mediating the evasion of the innate immune response since CPAF-deficient *Chlamydia* activate PMNs and are subsequently efficiently killed. CPAF suppresses the oxidative burst and interferes with chemical-mediated activation of neutrophils. We identified formyl peptide receptor 2 (FPR2) as a target of CPAF. FPR2 is cleaved by CPAF and released from the surface of PMNs. In contrast to previously described subversion mechanisms that mainly act on already activated PMNs, we describe here details of how *Chlamydia* actively paralyses PMNs, including the formation of neutrophil extracellular traps, to evade the host's innate immune response.**

Neutrophils are the most abundant innate immune cells and function by internalizing and killing microorganisms while at the same time secreting cytokines to recruit additional cells to amplify the innate immune response. When neutrophils encounter pathogens, they initiate their microbicidal armory to generate an oxidative burst and neutrophil extracellular traps (NETs), which are bactericidal DNA–protein aggregates that capture pathogens and thereby limit their spread[1]. Activation of neutrophils occurs following binding of pathogen-associated molecular patterns, such as formylated peptides, to surface-expressed receptors. Formylated peptides are specifically recognized by formyl peptide receptor 1 (FPR1), whereas another family member, FPR2, also known as ALX, is more promiscuous and binds other proteins, peptides and lipids[2,3]. A broad variety of microorganisms are known to activate neutrophils and induce the formation of NETs. As a response, pathogens have evolved mechanisms to degrade the extracellular chromatin traps by secreting effector nucleases and proteases[4].

C. trachomatis is an obligate intracellular human pathogen that is responsible for more than 131 million infections worldwide, making it the most common bacterial cause of sexually transmitted disease[5]. More than 60–80% of infections in women remain asymptomatic, which facilitates the spread of the pathogen and may subsequently develop into a chronic infection. Left untreated, *Chlamydia* infection increases the probability of co-infections with human immunodeficiency virus[6] and *Neisseria gonorrhoeae*[7].

Results

***C. trachomatis* infection prevents NET formation by human neutrophils**. In our efforts to better understand the interaction of *Chlamydia* and *N. gonorrhoeae* with phagocytes[8,9], we infected human neutrophils with these pathogens and investigated their response by microscopy to detect NET formation. Surprisingly, while infection of PMNs with *N. gonorrhoeae* or treatment with phorbol 12-myristate 13-acetate (PMA, which activates neutrophils) resulted in the formation of NETs, this did not occur when PMNs were infected with cleared lysates of *Chlamydia*-infected cells (Fig. 1a). Since co-infections of *C. trachomatis* and *N. gonorrhoeae* occur frequently and reach up to 40–50% in certain populations[10], we reasoned that *Chlamydia* infection may affect the interaction of *N. gonorrhoeae* with neutrophils, the major arm of the innate immune defence against gonococci[11]. We therefore exposed *Chlamydia* pre-infected neutrophils to *N. gonorrhoeae*. Interestingly, *Chlamydia* infection prevented the formation of NETs induced by *Neisseria* and also reduced the killing of *N. gonorrhoeae* by PMNs (Fig. 1b and Supplementary Fig. 1b), suggesting that *Chlamydia* infection prevents *Neisseria*-induced neutrophil activation, thereby supporting the survival of *N. gonorrhoeae* in PMNs. Closer inspection of the co-infected PMNs revealed that these cells appeared healthy and were packed with gonococci, indicating that they are fully competent for phagocytosis (Fig. 1b).

Chlamydia undergo an exclusive intracellular biphasic life cycle where the non-infectious replicative form, called the reticulate body (RB), differentiates into the non-replicative infectious elementary body (EB). When an infected epithelial host cell bursts to release the bacteria, the content of the inclusion is also discharged into the local environment. These EBs released from bursting cells are routinely used for experimental *Chlamydia* infections after removal of cellular debris (referred to as 'EB preparation'; for further details, see Methods). Interestingly, gradient-purified EBs depleted of material released by bursting host cells induced significantly more NETs than the EB preparations routinely obtained by clearing lysates of infected cells (Fig. 1c and Supplementary Fig. 1c,d). These gradient-purified EBs did not contain the secreted atypical serine protease CPAF[12] and exhibited only very low CPAF activity (Fig. 1d and Supplementary Fig. 1e,f) as previously reported[13]. Therefore, unless otherwise stated, EB preparations obtained by clearing lysates of infected cells were used for all infection experiments with *Chlamydia* derivatives.

[1]Department of Microbiology, Biocenter, University of Wuerzburg, Wuerzburg, Germany. [2]Present address: Department of Fundamental Microbiology, University of Lausanne, Lausanne, Switzerland. *e-mail: thomas.rudel@biozentrum.uni-wuerzburg.de

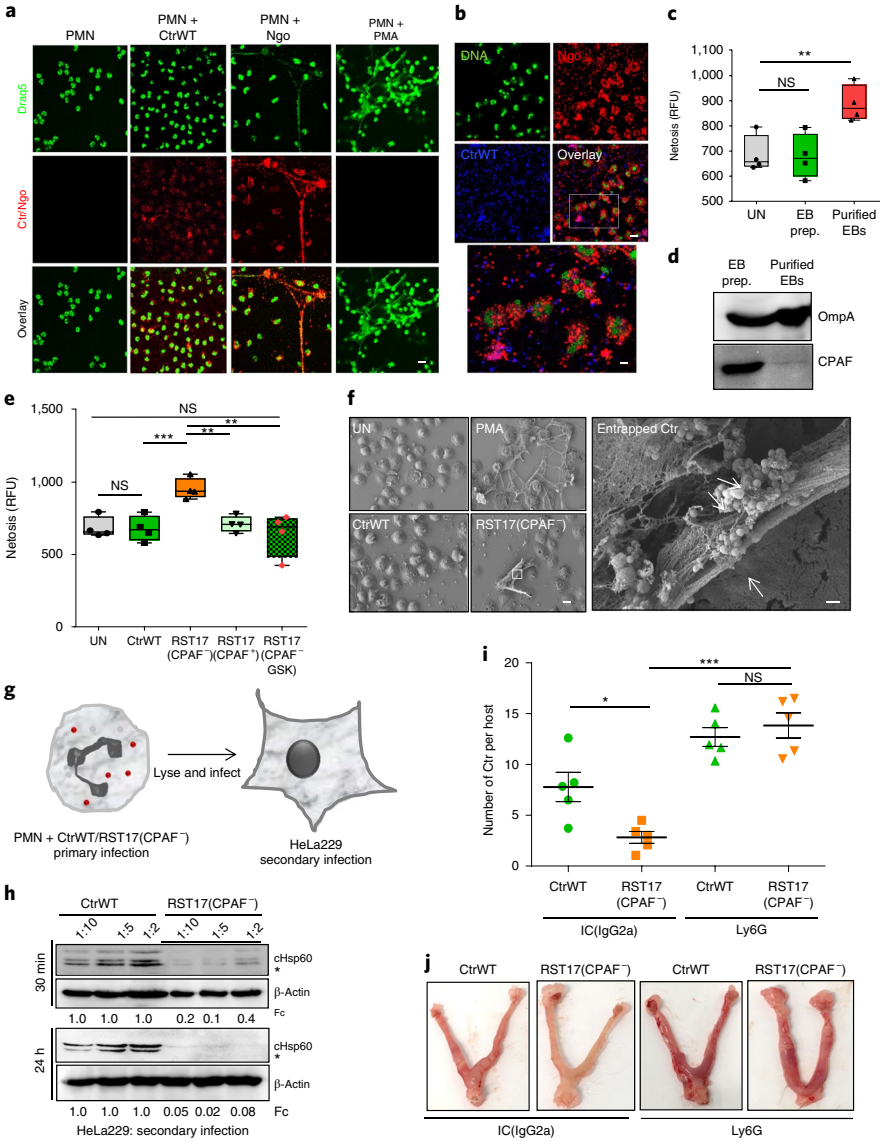

Fig. 1 | *Chlamydia trachomatis* prevents NET formation. a, Human neutrophils were isolated from healthy donors. The cells were either infected with CtrWT (MOI 10) or *N. gonorrhoeae* (Ngo; MOI 50) or treated with a known inducer of NETs (PMA: 25 ng ml^{-1}) for 4 h. The cells were fixed with 4% paraformaldehyde and stained for DNA (Draq5 (green) or bacteria (Ctr: anti-cHSP60/Ngo: anti-MOMP (red)). The stained cells were analysed by immunofluorescence microscopy. $n=3$. Scale bar, 20 µm. **b**, Human neutrophils seeded on glass slides were infected with wild-type *Chlamydia* (MOI 10) for 2 h and then co-infected with Ngo (MOI 50) for another 2 h. The cells were fixed and stained with Draq5 (stains DNA: green), anti-MOMP (stains Ngo: red) and anti-cHSP60 (stains Ctr: blue). $n=3$. Scale bars, 20 µm; enlarged overlay lowest picture: 1 µm. **c**, Human neutrophils were infected with either EB preparations (EB prep.) of CtrWT or Renografin-purified EBs for 4 h. The cells were analysed for NETs. The data are presented as box-and-whisker plots of four independent experiments in duplicate. $n=4$. $^{**}P<0.01$; NS, not significant (one-way ANOVA with Bonferroni's multiple-comparison test). UN, uninfected; RFU, relative fluorescence units. **d**, Western blot analysis of CPAF levels in EB preparations (EB prep.) and purified EBs of CtrWT. Chlamydial outer membrane protein A (OmpA) was detected as a loading control. $n=3$. **e**, The neutrophils from **a** together with RST17(CPAF^{-})-, RST5(CPAF^{+})- and RST17(CPAF-GSK)-infected cells were analysed for NET formation. Some of the data points are depicted in red to increase visibility. The data are presented as box-and-whisker plots of four independent experiments in duplicates. $n=4$. *P* values were determined by one-way ANOVA ($F=32.6$, $Df=3$) followed by a pairwise test with Bonferroni adjustment. $^{**}P<0.01$, $^{***}P<0.001$; NS, not significant. **f**, Neutrophils were infected with CtrWT or RST17(CPAF^{-}) or treated with PMA as described in **a** and analysed by scanning electron microscopy. $n=2$. Scale bars, 10 µm; enlarged picture on the right: 1 µm. **g**, Schematic diagram depicting how the infectivity assay was performed. Human neutrophils were infected with CtrWT or RST17(CPAF^{-}) at an MOI of 10 for 30 min/24 h (primary infection). The cells were then washed with PBS and lysed using glass beads. The supernatant was used to infect freshly plated HeLa229 cells (secondary infection). After 48 h, the cells were lysed and analysed via western blotting using antibodies against cHSP60 (Ctr infection marker) and β-actin (loading control). **h**, Secondary infection as depicted in **g**; the cells were lysed with Laemmli buffer and cHSP60 and β-actin were detected by western blot analysis. The asterisk indicates a nonspecific band. The intensities of the bands were normalized to β-actin and used to quantify the fold change (Fc) in bacterial infection. $n=3$. **i**, Chlamydial burden in neutropenic mice 7 days post-infection. The results are shown as the median ± the interquartile range of five mice per group in a single experiment. $n=5$. $^{*}P<0.05$, $^{***}P<0.001$; NS, not significant (one-way ANOVA with Newman–Keuls multiple-comparison test). **j**, Representative fallopian tubes of mice from **i** used to quantify *Chlamydia*. In each box plot, the whiskers denote minimum and maximum range of values and the horizontal line represents the median value.

***Chlamydia* CPAF is essential to survive PMN exposure.** CPAF is highly conserved between members of the Chlamydiaceae and has been identified as a pathogenicity factor, but its role in pathogenicity remains elusive. This protein exists as a zymogen in the bacterial cell and, on secretion into the inclusion lumen, it heterodimerizes, forming a potent protease[14] that is released into the surroundings when *Chlamydia* exit the lysed infected cell. Recent studies suggest that CPAF inhibits the complement activation pathway by degrading complement factor C3 and B[15]. CPAF is also known to degrade the antimicrobial peptides with anti-chlamydial activity[16] and promotes the survival of *C. trachomatis* in the lower genital tract of mice[17].

To further evaluate a possible role for CPAF in preventing NET formation, we tested a chlamydial strain with a nonsense mutation in the *cpa* gene that resulted in the expression of carboxy-terminally truncated and inactive CPAF[18]. We evaluated this CPAF mutant (RST17(CPAF$^-$))[18] for its capacity to cause PMN activation. Unlike wild-type *Chlamydia* (CtrWT), PMNs infected with RST17(CPAF$^-$) induced NETs (Fig. 1e,f). Since RST17(CPAF$^-$) contains additional mutations in the genome, an isogenic strain, RST5, which has the same background mutations but an intact *cpa* gene, was also used and behaved similarly in this assay to CtrWT (Fig. 1e). Furthermore, RST17(CPAF$^-$) complemented with a plasmid containing CPAF with a C-terminal GSK tag under the native promoter (RST17(CPAF–GSK)) behaved like CtrWT (Fig. 1e and Supplementary Fig. 1g). Since it has previously been shown that the RST17(CPAF$^-$) mutant is less infective towards epithelial cells[18], we infected PMNs with a range of infection doses from a multiplicity of infection (MOI) of 0.1 to 50 (Supplementary Fig. 2a,b). Even at a lower MOI, RST17(CPAF$^-$) induced significant NETs. We therefore focused on the role of CPAF in the interaction of *Chlamydia* with PMNs.

Chlamydia infection of epithelial cells is known to induce a robust cytokine and chemokine response that increases PMN infiltration into the infected area[19]. Thus, before entry into a new cell, EBs are exposed to PMNs whose function is to clear the infection[20]. To test whether *Chlamydia* are able to survive neutrophil attack, we exposed the wild type or RST17(CPAF$^-$) to PMNs and subsequently used the lysates from these PMNs to infect HeLa cells (Fig. 1g). Survival of CtrWT was increased during neutrophil attack compared to RST17(CPAF$^-$), even after an extended incubation period (Supplementary Fig. 2c,d). When using HeLa cells infected with neutrophil survivors as a source of pathogen for another round of infection (secondary infection), only CtrWT produced significant progeny, demonstrating that, in the absence of CPAF, neutrophils effectively clear the infection (Fig. 1h and Supplementary Fig. 3a,b).

Since the influence of CPAF on neutrophil activation could also be observed with purified mouse neutrophils (see below), we tested whether CPAF plays a similar important role in the defence against neutrophils in vivo by infecting control and neutropenic mice with CtrWT and RST17(CPAF$^-$). Ly6G antibody (1A8) was injected into C57BL/6 mice, which specifically depletes neutrophils without affecting other immune cell populations[21]. Within 24 h post-injection, 90% of neutrophils were depleted (Supplementary Fig. 4a,b). As previously shown[17], a CPAF-deficient strain was compromised in its ability to establish itself in the genital tract of control-injected mice whereas the bacterial load of CtrWT and RST17(CPAF$^-$) was similar in neutropenic mice (Fig.1i,j). This demonstrated that CPAF plays an important role in the defence against neutrophils in vivo.

***Chlamydia* infection interferes with neutrophil activation.** To investigate whether *Chlamydia* only survive or also multiply in PMNs, we infected PMNs with *Chlamydia* expressing GFP for different amounts of time and analysed the cells by western blots (Supplementary Fig. 3c), fluorescence-activated cell sorting (FACS; Supplementary Fig. 3d) and quantitative PCR (Supplementary Fig. 3e–g). Interestingly, all assays demonstrated that *Chlamydia* replicated and were biosynthetically active in PMNs. Since PMNs are short-lived cells, we initially considered that wild-type bacteria and CPAF could be cytotoxic and induce the killing of the PMNs, thereby increasing CtrWT survival. However, CtrWT infection rather prolonged the survival of neutrophils as shown by the increased β-actin levels in the infected versus the RST17(CPAF$^-$) or non-infected PMNs (Supplementary Fig. 2c, see the 24 h lane). Reduced cell death of PMNs even after 24 h of infection with CtrWT was also confirmed by propidium iodide staining (Fig. 2a). Strikingly, RST17(CPAF$^-$) increased PMN cell death already after 4 hours post-infection (hpi; Fig. 2b). To investigate whether the CPAF protease is responsible for the prolonged survival of PMNs, we generated recombinant purified CPAF (rCPAF) and recombinant catalytically inactive CPAF with a point mutation in the active site (rCPAF*) (Supplementary Fig. 5a). Increased cell death and netosis (NET-associated killing) induced by RST17(CPAF$^-$) infection was prevented by the addition of rCPAF, but not by rCPAF* (Fig. 2b,c), indicating that CPAF directly affects the survival of PMNs.

Reactive oxygen species (ROS) produced by neutrophils following activation elicit direct bactericidal activity and are required for the formation of NETs[22]. We next asked whether CtrWT could prevent ROS and NET production as well as the upregulation of the activation marker CD11b induced by the potent PMN activator PMA. PMNs pre-infected with CtrWT or RST17(CPAF$^-$) were subsequently challenged with PMA. Interestingly, CtrWT, but not RST17(CPAF$^-$), efficiently blocked PMA-induced NET and ROS production as well as the exposure of the activation marker CD11b in neutrophils (Fig. 2d–f). Since protein kinase C (PKC) activation is difficult to detect in primary neutrophils, we made use of neutrophil-like HL60 cells to investigate the downstream signalling pathways. CtrWT infection prevented both basal and PMA-induced PKC activation (Fig. 2g), further indicating that CPAF interferes with the activation of PMNs. These data demonstrate that *Chlamydia* prevent the activation of PMNs in a CPAF$^-$dependent way to enhance their survival in the extracellular environment.

FPR2 is a critical target of CPAF. The natural activation of PMNs in response to pathogen occurs via surface receptors, most prominently by formyl peptide receptors (FPR1 and FPR2). To reveal whether *Chlamydia* manipulate neutrophils at the level of surface receptors, we challenged infected neutrophils with the specific FPR1 agonist fMLP. Calcium mobilization is an early signalling event after FPR activation and a prerequisite for neutrophil activation[23]. Treatment of PMNs with fMLP elicited Ca^{2+} signalling in both CtrWT- and RST17(CPAF$^-$)-infected cells (Fig. 3a). This demonstrated that FPR1 receptor-mediated signalling remains intact also in the presence of CtrWT. By contrast, the FPR2-specific agonist MMK1 failed to mobilize calcium in the presence of CtrWT (Fig. 3b), indicating that the pathogen impairs FPR2 receptor-mediated activation. We next investigated whether CtrWT or RST17(CPAF$^-$) infection of PMNs affected the surface exposure of FPR1 and FPR2 (Fig. 3c,d). Unlike FPR1, while FPR2 levels increased following infection of PMNs with RST17(CPAF$^-$), they did not increase following CtrWT infection (Fig. 3c,d). This effect of FPR2 depletion on the surface of neutrophils was dependent on the protease activity of CPAF, since an active recombinant CPAF (rCPAF), but not a catalytically inactive recombinant CPAF (rCPAF*), effectively reduced FPR2 surface levels (Supplementary Fig. 5b). To understand whether CPAF directly targets FPR2, neutrophils treated with rCPAF or rCPAF* were subjected to calcium flux analysis following treatment with the agonists fMLP and MMK1. Treatment of PMNs with rCPAF interfered with calcium fluxes induced by MMK1, but not by fMLP, further supporting the hypothesis that CPAF specifically interferes with FPR2 function on the cell surface (Fig. 3e). Furthermore, the reduction in FPR2

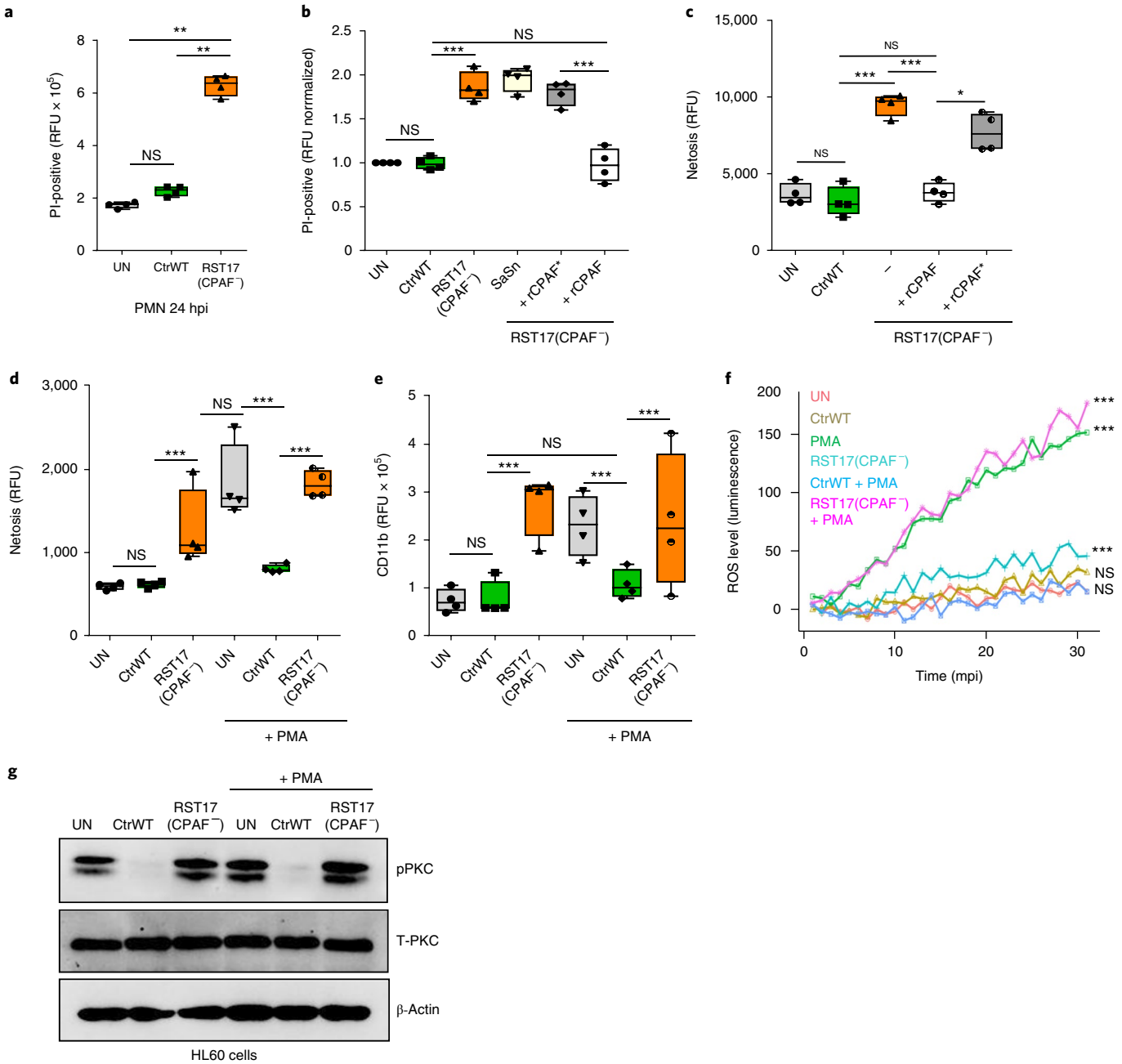

Fig. 2 | *Chlamydia* abrogates receptor-independent activation of neutrophils. a, Human neutrophils were infected with CtrWT/RST17(CPAF⁻) (MOI 10, 24 h). The cells were stained with propidium iodide (PI) to determine cell death. The *P* values were determined by one-way ANOVA with Bonferroni's multiple-comparison test. $n = 4$. The data are presented as box-and-whisker plots of four independent experiments in duplicates. **b**, Human neutrophils were infected with CtrWT/RST17(CPAF⁻) or treated with supernatant of *Staphylococcus aureus* cultures as a positive control (SaSn). RST17(CPAF⁻) was treated with active/inactive recombinant CPAF (rCPAF/rCPAF*), before infecting neutrophils. The cells were stained with propidium iodide 4 hpi. The *P* values were determined by one-way ANOVA ($n = 4$, $F = 18.84$, Df = 5) followed by a pairwise test with Bonferroni adjustment. **c**, Netosis was determined in neutrophils infected as in **b**. The *P* values were determined by one-way ANOVA ($n = 4$, $F = 24.39$, Df = 4) followed by a pairwise test with Bonferroni adjustment. **d**, Human neutrophils either left untreated or infected with CtrWT or RST17(CPAF⁻) for 30 min were further challenged with PMA (10 ng ml^{-1}) for 3.5 h before analysis of netosis. The *P* values were determined by one-way ANOVA ($n = 4$, $F = 31.47$, Df = 5) followed by a pairwise test with Bonferroni adjustment. **e**, Cells infected and treated as in **d** were stained for cell surface expression of CD11b and analysed using FACS. The *P* values were determined by one-way ANOVA ($F = 31.47$, Df = 5) followed by a pairwise test with Bonferroni adjustment. $n = 4$. **f**, Human neutrophils were left uninfected or infected with CtrWT or RST17(CPAF⁻) and challenged with PMA. Total ROS generated by neutrophils over 30 min was determined. The data are represented at each time as the mean. The *P* values were determined using multiple regressions by fitting the data to a linear model ($n = 3$, $F = 56.35$, Df = 35 and 522, adjusted $R^2 = 0.77$). mpi, minutes post-infection. **g**, HL60 cells were infected with CtrWT or RST17(CPAF⁻) at an MOI of 10 for 30 min and challenged with PMA for 3.5 h. The cells were analysed by western blotting for pPKC and total PKC (T-PKC). β-actin serves as the loading control. $n = 3$, $^*P < 0.05$, $^{**}P < 0.01$, $^{***}P < 0.001$; NS, not significant. In each box plot, the whiskers indicate the minimum and maximum range of values and the horizontal line represents the median.

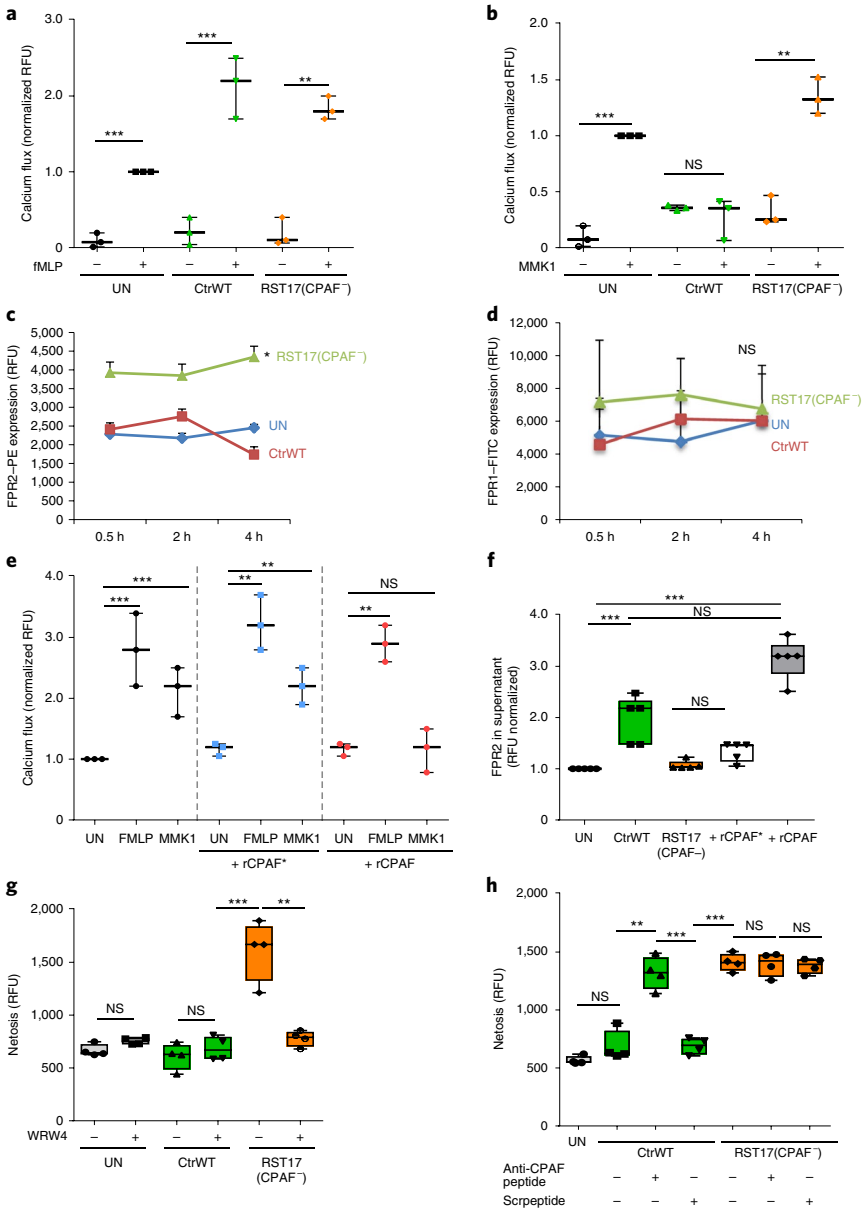

Fig. 3 | The *Chlamydia* effector CPAF targets FPR2. a,**b**, Fluo-3-Am-stained human neutrophils were left uninfected or infected with CtrWT or RST17(CPAF⁻) (MOI 10, 30 min). The cells were stimulated with the FPR1 agonist fMLP (1 nM) (**a**) or the FPR2 agonist MMK1 (62.5 nM) (**b**), and calcium mobilization was measured using FACS. $n=3$. *P* values were determined by one-way ANOVA ($F=55.3$ and 49.76, Df = 17 and 17, respectively) followed by a pairwise test with Bonferroni adjustment. The results are shown as dot plots with the minimum and maximum range of values, the horizontal line represents the median. $^{**}P<0.01$, $^{***}P<0.001$; NS, not significant. **c**, Human neutrophils were left uninfected or infected with CtrWT/RST17(CPAF⁻) for different time points. The cells were stained with PE-conjugated FPR2 antibody, and the kinetics of FPR2 expression on the cell surface was measured using FACS. **d**, The cells from **c** were stained with FITC-conjugated FPR1 antibody, and the kinetics to FPR1 expression on the cell surface was measured using FACS. $n=3$. The data shown in **c** and **d** are presented as mean ± standard deviation. The *P* values for both FPR1 and 2 were determined by the Durbin and Conover method with a pairwise post hoc test. $^{*}P<0.05$; NS, not significant. **e**, Fluo-3-Am-stained human neutrophils were left untreated or treated with active/inactive recombinant CPAF (rCPAF/rCPAF*). These cells were further stimulated with the FPR1 and FPR2 agonists fMLP and MMK1, respectively. The relative fluorescence was measured using FACS and normalized to buffer controls. $n=3$. The *P* values were calculated by one-way ANOVA ($F=19.49$, Df = 26) followed by a pairwise test with Bonferroni adjustment. The data are shown as a dot plot, with the minimum and maximum range of values and the horizontal line represents the median. $^{**}P<0.01$, $^{***}P<0.001$; NS, not significant. **f**, Human neutrophils were infected with CtrWT/RST17(CPAF⁻) (MOI 10) or treated with rCPAF/rCPAF* for 4 h. The supernatant was collected and analysed for the presence of FPR2 using ELISA. The *P* values were determined by one-way ANOVA ($n=5$, $F=48.37$, Df = 24) followed by a pairwise test with Bonferroni adjustment. $^{***}P<0.001$; NS, not significant. **g**, Human neutrophils were treated with the inhibitor of FPR2, WRW4, for 1 h as indicated. The cells were then washed and infected with CtrWT or RST17(CPAF⁻) for 3 h. The mean netosis rate was calculated. $n=3$, $^{***}P<0.001$, $^{**}P<0.01$; NS, not significant (one-way ANOVA with Bonferroni's multiple-comparison test). **h**, Human neutrophils were infected with CtrWT/RST17(CPAF⁻) treated with anti-CPAF peptide or scrambled (Scr) peptide for 4 h and then subjected to netosis assay. The *P* values were determined by one-way ANOVA ($n=4$, $F=12.69$, Df = 6) followed by a pairwise test with Bonferroni adjustment. $^{***}P<0.001$, $^{**}P<0.01$; NS, not significant. The data in **f**–**h** are presented as box plots, the whiskers indicate the minimum and maximum range of values and the horizontal line represents the median.

protein expression in neutrophils infected with CtrWT compared to infection with mutant bacteria (Supplementary Fig. 5c) occurred in the absence of any changes in FPR2 transcript levels (Supplementary Fig. 5e). Taken together, these results pointed to a direct processing of FPR2 by CPAF, and in agreement with this, FPR2 was detected by enzyme-linked immunosorbent assay (ELISA) in the supernatant of CtrWT-infected and rCPAF-treated neutrophils (Fig. 3f). ELISA specifically detected the second extracellular loop of FPR2 (peptide Phe163 to Arg205), indicating that this peptide is released from FPR2 by CPAF. To detect whether FPR2 serves as a direct target of CPAF, we incubated recombinant FPR2 with different concentrations of rCPAF. Similarly to a previously described in vitro substrate of CPAF, vimentin[24], FPR2 was also cleaved by recombinant CPAF, in the lowest used CPAF concentration (Supplementary Fig. 5f). We also used the specific FPR2 antagonist WRW4[25], which prevented FPR2-mediated intracellular calcium flux, superoxide generation and chemotactic migration of neutrophils[25]. WRW4 rescued NET formation when incubated with RST17(CPAF$^-$) (Fig. 3g). Thus, our data demonstrate that *Chlamydia* hijack neutrophils by specifically targeting FPR2.

To further substantiate that CPAF is responsible for inhibiting FPRs, we designed cell-impermeable peptides against CPAF[26]. The anti-CPAF peptide blocked CPAF activity since it prevented the processing of the known CPAF in vitro substrate vimentin (Supplementary Fig. 5a). Incubation of CtrWT with the CPAF inhibitory peptide resulted in the activation of neutrophils as shown by increased netosis rates (Fig. 3h), supporting a direct role for protease activity in silencing neutrophil activation. Consistently, when RST17(CPAF$^-$) was treated with active rCPAF and inhibitory peptide, the bacteria still activated netosis (Supplementary Fig. 5g). Neither the anti-CPAF nor the scrambled peptide alone showed any effect on PMN netosis (Supplementary Fig. 5h). Taken together, these data strongly support a direct role for the active protease in preventing the activation of neutrophils.

***Chlamydia* infection interferes with FPR signalling.** Investigating the FPR downstream signalling in HL60 cells revealed that RST17(CPAF$^-$), but not CtrWT, activated MAP-kinase (MAPK) and phosphatidylinositol-3-OH kinase (PI(3)K) signalling (Fig. 4a). Both, PKC activation[27] and Raf/MAP-kinase kinase (MEK)/ERK signalling[28] are critical for the generation of NETs, and inhibition of these downstream signalling pathways strongly interfered with NETs induced by RST17(CPAF$^-$) (Fig. 4b). This demonstrated that CtrWT utilizes CPAF to dampen FPR signalling to prevent the activation of neutrophils.

On sensing microorganisms, neutrophils transmigrate rapidly to the site of infection. This is facilitated by the extension of lamellipodia and filopodia, which we observed 1 min after infection with RST17(CPAF$^-$), while neutrophils infected with CtrWT remained indistinguishable from uninfected control cells. This indicated that CPAF interferes with neutrophil polarization (Supplementary Fig. 6a). To more comprehensively characterize the defect of PMNs challenged with *Chlamydia*, we investigated other aspects of their antibacterial responses, including degranulation as a measure of their bactericidal activity, production of pro-inflammatory cytokines as readout for immune stimulatory behaviour, and chemotaxis as a measure for detection at infection sites. CPAF-deficient, but not wild-type, *Chlamydia* induced these typical PMN antibacterial responses (Fig. 4c–f and Supplementary Fig. 6b,c).

FPR2 is required to limit replication of CPAF-deficient *Chlamydia* in vivo. To demonstrate a role for FPR2 in the defence against *Chlamydia* infection, neutrophils from C57BL/6 control and FPR2 knockout (FPR2-KO) mice (Supplementary Fig. 7a–c) were purified and exposed to *Chlamydia*. RST17(CPAF$^-$) induced significantly higher levels of netosis in mouse neutrophils compared to CtrWT and RST17(CPAF–GSK) (Fig. 5a). Neutrophils from FPR2-KO animals did not respond differently when infected with CPAF-expressing or -deficient strains (Fig. 5b). The survival rate of *Chlamydia* in the PMNs from C57BL/6 control and FPR2-KO mice mirrored this trend (Fig. 5c,d). We then infected C57BL/6 control mice by transcervical injection with CtrWT, RST17(CPAF$^-$) or RST17(CPAF–GSK) strains. The CPAF-deficient strain was less able to establish itself in the fallopian tubes of mice, which was rescued by expression of CPAF on a plasmid in RST17(CPAF–GSK) (Fig. 5e,f). Interestingly, when FPR2-KO mice were infected with CtrWT or RST17(CPAF$^-$), the bacterial load did not change significantly (Fig. 5e,f). This identifies FPR2 as a key factor in controlling *Chlamydia* infection in vivo. Thus, our data demonstrate that the secreted protease CPAF broadly paralyses PMNs and constitutes a major factor involved in immune escape during *Chlamydia* infection.

Discussion

C. trachomatis is known to cause asymptomatic infection that may have severe consequences since, if untreated, it may lead to a chronic state. Although previous studies have demonstrated that *Chlamydia* infection interferes with individual steps in cell-autonomous and innate immune signalling pathways, the mechanism of general immune escape has remained unknown. Here we show that free *Chlamydia* do not activate PMNs even on direct interaction. Once PMNs engage *Chlamydia*, these neutrophils are paralysed and fail to respond to activation by different stimuli. In this study, we have identified the secreted chlamydial serine protease, CPAF, as the central effector involved in evading PMNs, the first line of host innate immune defence. We therefore propose that CPAF-mediated inactivation of PMNs is a crucial event in asymptomatic *C. trachomatis* infection.

The initial observation that *Chlamydia* do not induce NETs on interaction with PMNs was an intriguing finding since previous reports demonstrate that numerous diverse pathogens induce NET formation by neutrophils[1,29]. *Chlamydia* infection induces IL-8 secretion in epithelial cells[30], which attracts neutrophils, leading to their increased influx to the site of infection[31]. However, despite this increased number of neutrophils at the site of *C. trachomatis* (MoPn: mouse pneumonitis biovar) infection, they are not able to clear the infection in mice[32,33]. This is in contrast to the expectation that PMNs would limit *Chlamydia* spreading once the bacteria leave the host cell after completing a replication cycle. Transition from the lysed host cell to the next suitable intact host cell for the subsequent replication cycle is not only crucial for the propagation of the bacteria but it is also critical since the bacteria are fully exposed to the host's innate and adaptive immune defence. Our experiments have demonstrated that *Chlamydia* overcome this barrier, evade PMNs and remain competent to infect fresh cells and produce progeny (Fig. 1h and Supplementary Fig. 2c). They even replicate in PMNs and produce infectious progeny. However, the capacity to replicate in PMNs is not required for immune evasion, since wild-type in contrast to CPAF-deficient *Chlamydia* exposed for only 30 min to PMNs—a time span too short for replication—were able to survive and produce progeny in epithelial cells. This demonstrates that evasion of PMN-mediated innate immunity crucially depends on CPAF.

Detection of microbial products results in the activation of innate signalling pathways and the formation of NETs. This also leads to a variety of effector mechanisms including degranulation, increased migration and ROS production, the last of which induces NET formation. The strong depletion of ROS activation was not due to the degradation of the reduced nicotinamide adenine dinucleotide phosphate (NADPH) oxidase complex (Fig. 2f and Supplementary Fig. 3h). *Chlamydia* prevented all of these consequences of PMN activation and thus clearly acts upstream and before NET formation.

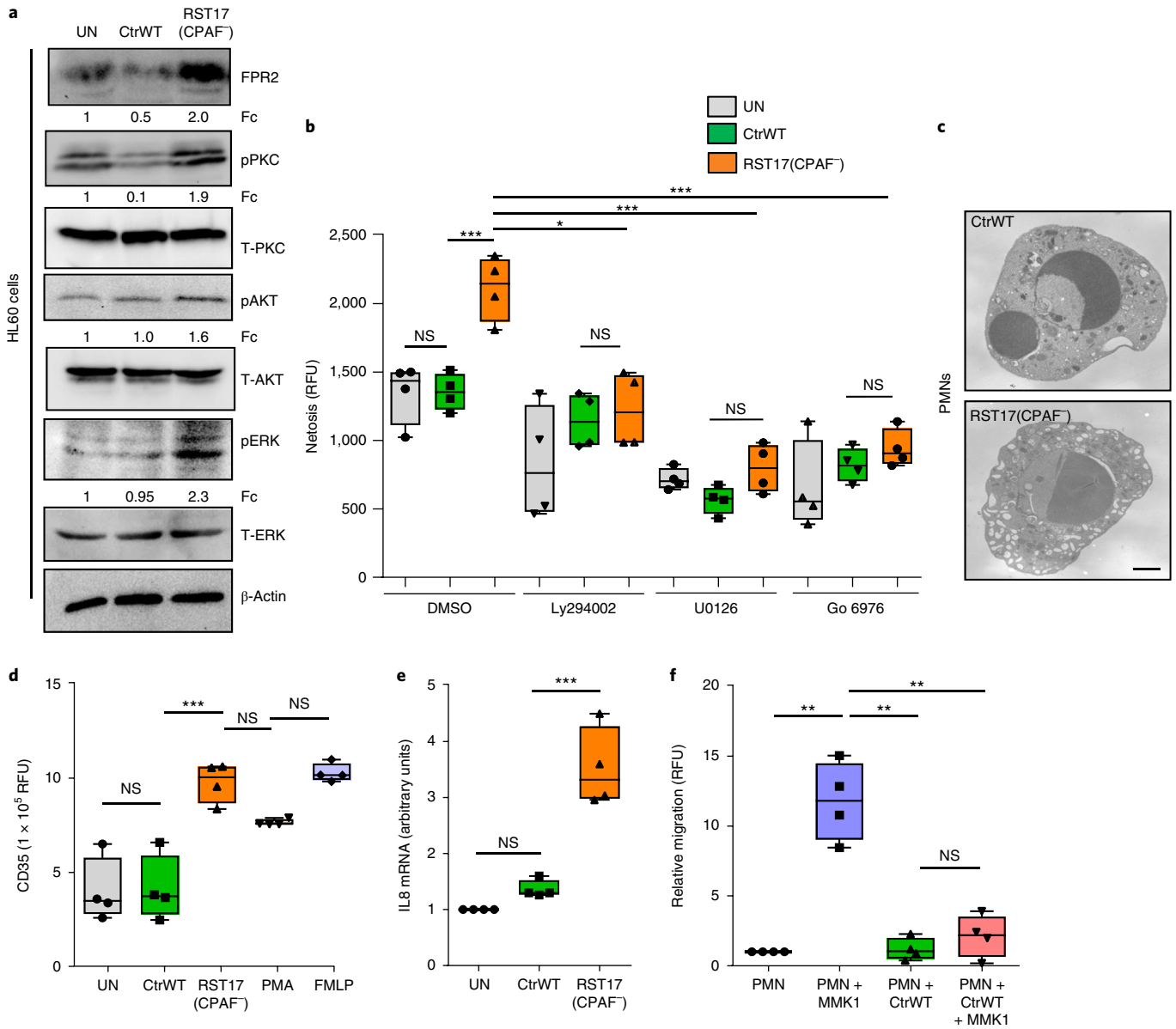

Fig. 4 | *Chlamydia* infection dampens G-protein-coupled receptor signalling and prevents neutrophil degranulation. a, HL60 cells were infected with CtrWT/RST17(CPAF⁻) (MOI 10, 4 h). The cells were lysed and analysed using western blotting for FPR2, pPKC, total PKC (T-PKC), pAKT, total AKT (T-AKT), pERK, total ERK (T-ERK) and β-actin. Fold change (Fc) normalized to the uninfected control and/or the total kinase versus phosphorylated kinase is indicated directly below the blots. The blots represent three independent experiments with similar results ($n=3$). **b**, Human neutrophils (5×10^5 cells) were treated with the vehicle DMSO (dimethylsulfoxide) or the PI(3)K inhibitor (LY294002 10 μM), MAPK inhibitor (U0126 10 μM) and PKC inhibitor (Go 6976 200 nM) for 30 min. The cells were infected with CtrWT/RST17(CPAF⁻) for 4 h and netosis rates were determined. The *P* values were determined by one-way ANOVA ($n=4$, $F=14.61$, Df = 47) followed by a pairwise test with Bonferroni adjustment. $^*P<0.05$, $^{***}P<0.001$; NS, not significant. **c**, Human neutrophils were infected with CtrWT/RST17(CPAF⁻) (MOI 10) and processed for transmission electron microscopy. The feature of strong degranulation is visible by increased granules and vacuoles. The images represent two independent experiments with similar results ($n=2$). Scale bar, 1 μm. **d**, Human neutrophils were infected with CtrWT/RST17(CPAF⁻) (MOI 10) and then stained for surface expression of CD35, a marker protein for exocytosis of secretory vesicles. *P* values were determined by one-way ANOVA ($n=4$, $F=24.35$, Df = 19) followed by a pairwise test with Bonferroni adjustment. $^{***}P<0.001$; NS, not significant. **e**, IL-8 expression was determined by RT–PCR with RNA isolated from infected human neutrophils and calculated as fold change normalized to levels of uninfected cells. *P* values were determined by one-way ANOVA ($n=4$, $F=42.29$, Df = 11) followed by a pairwise test with Bonferroni adjustment. $^{***}P<0.001$; NS, not significant. **f**, Neutrophils were stained with CFSE, either left uninfected or infected with CtrWT and subjected to a chemotaxis assay with MMK1 in the lower chamber. After 1 h, the fluorescence in the lower chamber was measured, which corresponds to the rate of migration. The *P* values were determined by one-way ANOVA ($n=4$, $F=39.68$, Df = 15) followed by a pairwise test with Bonferroni adjustment. $^{**}P<0.01$; NS, not significant. In each box plot, the whiskers indicate the minimum and maximum range of values and the horizontal line represents the median.

We therefore argue that *Chlamydia* actively prevents activation. This is in line with the broad and robust suppression of immune responses that one would expect as a mechanism underlying asymptomatic infections.

Our search for possible CPAF targets that could explain the effect *Chlamydia* have on PMNs revealed that FPR2 is cleaved and released into the culture supernatant. Interestingly, in contrast to FPR2, the related FPR1 remains intact in infected cells and

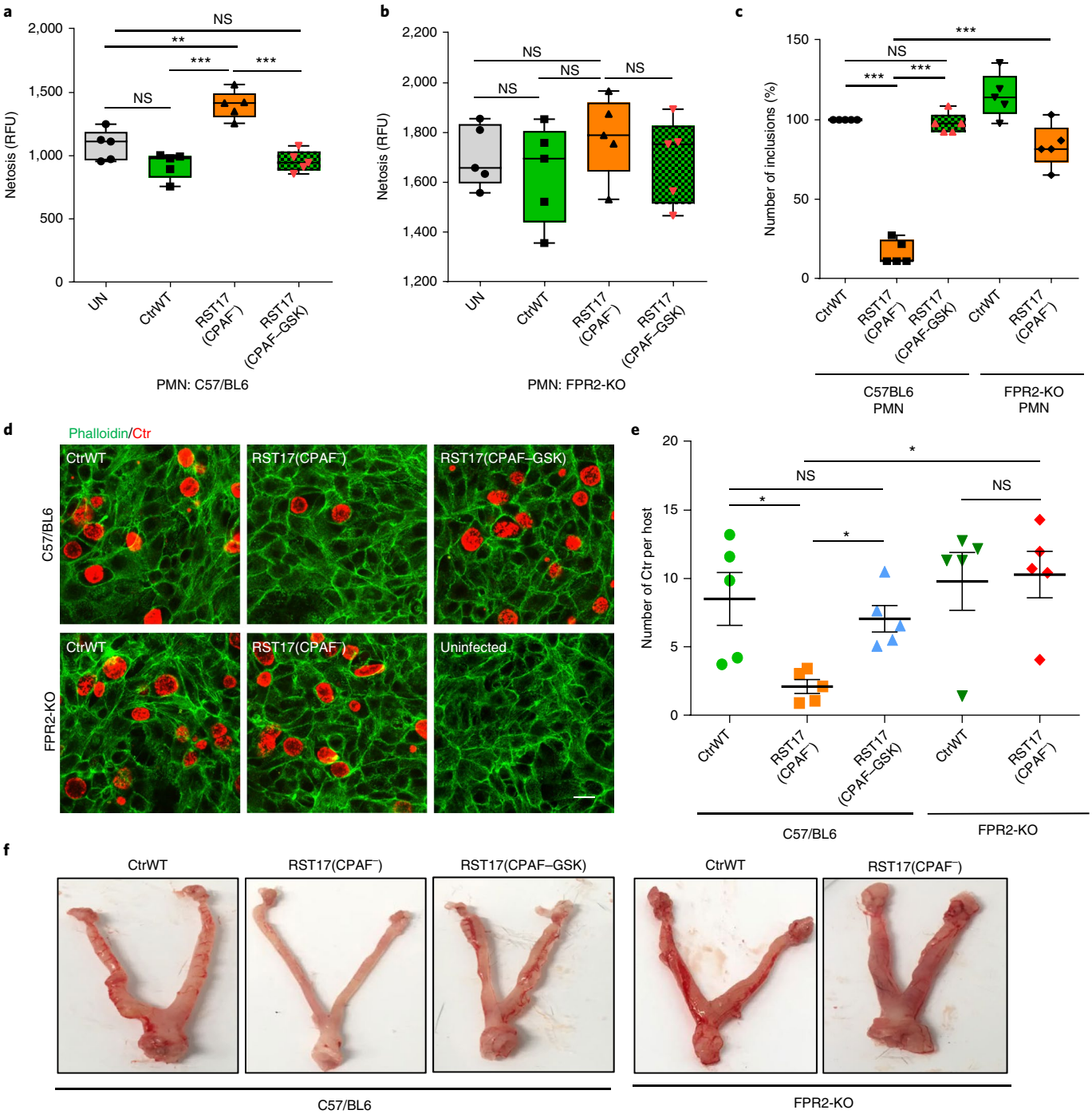

Fig. 5 | FPR2-KO mice rescue the survival of CPAF-deficient *Chlamydia*. **a**,**b**, Neutrophils were isolated from the bone marrow of five C57/BL6 and FPR2-KO mice. PMNs were infected with CtrWT, RST17(CPAF⁻) or RST17(CPAF–GSK) for 4 h and then subjected to netosis assays. Some of the data points are depicted in red to increase visibility. Significance was calculated using one-way ANOVA with a Bonferroni multiple-comparison test; $F = 21.04$, Df = 19; $F = 0.664$, Df = 19. The data are presented as box-and-whisker plots of PMNs isolated from five mice, tested in triplicate in a single experiment. $^{**}P < 0.01$, $^{***}P < 0.001$; NS, not significant. $n = 5$. **c**, Infected neutrophils from **a**,**b** were washed and lysed to infect freshly plated HeLa cells. The number of inclusions was counted from five different microscopic fields. The percentage of inclusions was calculated by normalizing to the number of inclusions counted in cells infected with CtrWT obtained from infected C57/BL6 PMNs. Some of the data points are depicted in red to increase visibility. The data are presented as box-and-whisker plots of three independent experiments in duplicate. $n = 3$. $^{***}P < 0.001$; NS, not significant. Significance was calculated using one-way ANOVA with a Bonferroni multiple-comparison test; $F = 77.59$, Df = 24. **d**, Images from **c** obtained 48 hpi. The cells were stained for *Chlamydia* (cHSP60: red) and cells (phalloidin: green). Scale bar, 20 µm. **e**, C57/BL6/FPR2-KO mice were infected with CtrWT, RST17(CPAF⁻) or RST17(CPAF–GSK) for 7 days. The bacterial burden was calculated and the results are presented as median ± the interquartile range of five mice per group in a single experiment. $^{*}P < 0.05$ (one-way ANOVA with Newman–Keuls multiple-comparison test); NS, not significant. **f**, Representative fallopian tubes of mice from **e** used to quantify *Chlamydia*.

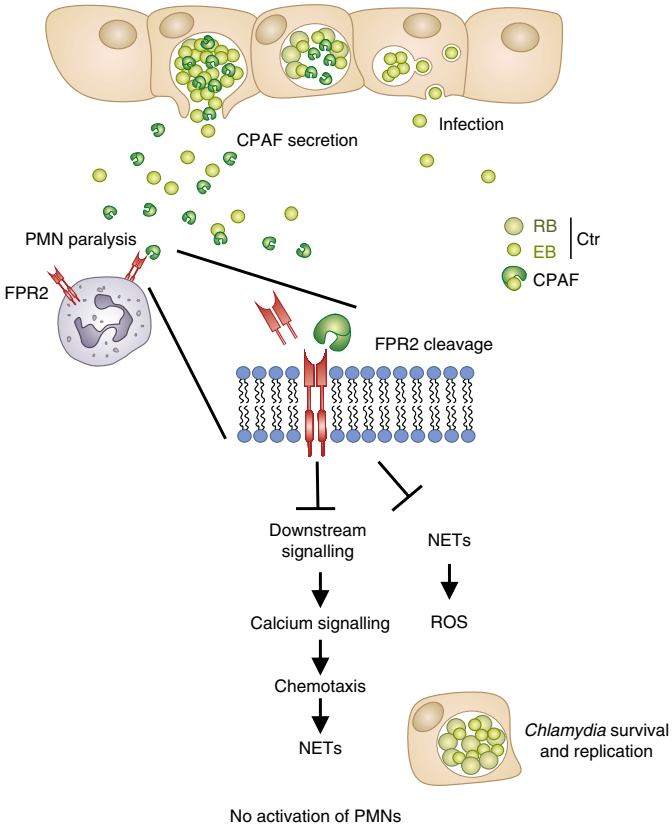

Fig. 6 | Model of human neutrophil paralysis by *Chlamydia* infection. *Chlamydia*, on release from the host epithelial cells, encounters neutrophils, the first line of immune defence. The neutrophils come into contact with the secreted effector protease CPAF of *Chlamydia*. The FPR2 present on the surface of neutrophils is targeted by CPAF. This dampens G-protein-coupled receptor signalling, further preventing the downstream activation of neutrophils and enabling pathogen survival.

is capable of mediating ligand-dependent calcium signalling. However, FPR1 signalling pathways appear not to be activated in infected neutrophils. Consistent with a role for CPAF in the specific processing of the receptor, recombinant active CPAF efficiently trimmed FPR2 (Fig. 3f and Supplementary Fig. 5b,c,f) and rescued the phenotype of RST17(CPAF^{-}) (Fig. 2b,c). Likewise, inhibiting CPAF activity during infection of PMNs with wild-type bacteria protected FPR2 from processing (Supplementary Fig. 5d). We thus propose that FPR2 is a critical target of CPAF to prevent PMN activation in the context of *Chlamydia* infection.

However, the data presented on the downregulation of PMN activation cannot be explained solely by the processing of FPR2. A broad range of stimuli failed to activate PMNs in the presence of CtrWT, including the PKC activator PMA and *N. gonorrhoeae*, a pathogen frequently observed as co-infecting patients with *Chlamydia* infection. A potential role for CPAF in processing targets in the cytosol of host cells is currently still debated[34]; it is even possible that the protease acts on the bacteria themselves, reducing the surface exposure of peptides and thus dampening the immune response. Although the full understanding of the role of CPAF in the downregulation of the response of neutrophils requires further studies, on the basis of our in vitro and in vivo data, we propose the following model (Fig. 6). During their developmental cycle, *Chlamydia* secrete CPAF into the inclusion lumen where it is activated. After completion of the cycle, the host cell lyses and releases the EBs together with the active CPAF. Released CPAF cleaves FPR2 and probably other targets, such as Toll-like receptors, which been implicated in the activation of PMNs[35], thereby paralysing PMNs locally at the site of infection. Consequently, the EBs avoid eradication during their passage from one host cell to a new host cell. Considering the potential central role of CPAF outside the infected cells, it is tempting to speculate that CPAF inhibitors could function as new therapeutics against *Chlamydia* infection. This is supported not only by the reduced survival of CPAF mutants in a mouse genital infection model[17] (Figs. 1i,j and 5e,f), but also by the observation that inhibitory peptides directed against CPAF mediate destruction of *Chlamydia* by PMNs (Fig. 3h and Supplementary Fig. 5g,h). Hence, an in-depth understanding of the strategies that *Chlamydia* utilizes to paralyse the host innate immune system could reveal therapeutic interventions to tackle this silent epidemic.

Methods

Ethics statement. Venous blood from healthy human individuals was obtained with informed consent signed by the volunteers. Use of human blood and neutrophils was approved by the Ethics Commission of the University of Wuerzburg (Code 2015091401). Animal studies were approved by the local government of Franconia, Germany (approval no. 55.2-2531.01-49/12) and performed in strict accordance with the guidelines for animal care and experimentation of German Animal Protection Law.

Chlamydial strain and cell types. *Chlamydia trachomatis* L_2 (strain L_2/434/Bu) was used in this study. *Chlamydia* was propagated as described in ref. [36]. *Chlamydia* EBs were verified to be free of *Mycoplasma* contamination via PCR. The *Homo sapiens* cervix adenocarcinoma cell line HeLa229 (ATCC CCL-2.1) was used to test *Chlamydia* for deficiency of CPAF and the inhibitory activity of peptides against CPAF. HL60 cells stably transfected with human FPR1 or FPR2/ALX[37,38] were used in the study. Both of these cell lines were grown in RPMI medium (Gibco) supplemented with 10% FCS (Biochrome). Transfected cells were grown in the presence of G418 (Invitrogen) at a final concentration of 1 mg ml^{-1}. Cell cultures were grown and maintained at 37 °C in a humidified tissue culture incubator with 5% CO_2 using standard tissue culture procedures.

The cell line from ATCC (HeLa229) was authenticated by ATCC and was not further validated in our laboratory. HL60 cells (originally from ATCC) were obtained from D. Kretschmer and A. Peschel (Universität Tübingen, Germany) and were not validated further in our laboratory. All cell lines were tested for the presence of mycoplasma and were mycoplasma free.

Preparation of clear lysate of *Chlamydia*. *Chlamydia trachomatis* was grown in HeLa229 cells. The cells were lysed after 48 hpi using glass beads (2.85–3.45 mm). The cell debris was removed by centrifuging at 2,000 *g*. for 10 min at 4 °C. The supernatant was collected and centrifuged at 24,000 *g* for 30 min at 4 °C. The pellet was resuspended in sucrose–phosphate–glutamic acid (SPG; 10 mM sodium phosphate (8 mM $Na_2HPO_4^-$, 2 mM NaH_2PO_4), 220 mM sucrose, 0.50 mM L-glutamic acid) buffer and passed through G20 and G18 syringes to dissociate clumps. The bacteria were aliquoted and frozen at −80 °C until use (Supplementary Fig. 1d).

Purification of EBs. *Chlamydia trachomatis* was grown in HeLa229 cells for 48 h. The cells were then lysed using glass beads (2.85–3.45 mm) and centrifuged at 2,000 *g* for 10 min. EBs/RBs were sedimented by centrifugation at 24,000 *g* for 30 min. The supernatant was discarded and the pellet was suspended in 3.0 ml of Hank's balanced salt solution, and loaded on a 20%–50% (vol/vol) Renografin gradient in high-speed centrifugation tubes. The gradient was further centrifuged at 60,000 *g* for 1 h at 4 °C in a swinging bucket rotor. EBs were visible as a turbid tan gummy disc. The upper layer was carefully aspirated and the EB layer was further washed and resuspended in SPG buffer. The purity of the EBs was confirmed by electron microscopy (Supplementary Fig. 1c).

Mice used in the study. FPR2-deficient (KO) mice were obtained from O. Söhnlein (Institute of Prophylaxis and Epidemiology of Circulatory Diseases, Ludwig-Maximilians-University Munich, Germany) and originated from J. M. Wang (NCI, CCR Maryland, USA)[39]. The FPR2-KO mice have a C57BL/6 background; hence, the control infection was carried out in C57BL/6 mice.

Transcervical mouse infections and determination of bacterial burden. All animal experiments were performed in accordance with protocols approved by animal care and experimentation of German Animal Protection Law approved under the Animal (Scientific Procedures) Act 1986 (project licence 55.2-2531.01-49/12). Female mice older than 8 weeks were used for the study. Five days before transcervical infection, mice were treated subcutaneously with 2.5 mg of DepoProvera (medroxy-progesterone acetate). The mice were transcervically infected with 1×10^7 infection-forming units of Ctr using a non-surgical embryo transfer device (ParaTechs Corp.). Uninfected mice were treated the same way by

injecting SPG buffer (vehicle) transcervically.
The mice were euthanized 7 days post-infection and the uterine horns were taken for further analysis. The uterine horns were homogenized in SPG buffer and DNA was isolated using DNeasy blood and tissue kit (Qiagen). Quantitative PCR was used to enumerate *Chlamydia* and host genome copy number.
The following primers were used for amplifying the *C. trachomatis lytA* gene that was cloned into the vector: fwd, 5′-TCTAAAGCGTCTGGTGAAAGCT-3′ and rev, 5′-GAAATAGCGTAGTAATAATACCCG-3′. Normalization of bacterial genome to that of the host was performed using mouse synectin primers: fwd, 5′-ACTAATGTCAAGGAGCTGTACG-3′ and rev, 5′-CCTCCGACTTGAACACTTCC-3′. Quantitative PCR with reverse transcription (RT–PCR) was performed as described below. Data were analysed using Step One Plus software package (Applied Biosystems) and expressed as the ratio of chlamydial genome to host genome (*lytA*/synectin). GraphPad Prism 7 was used to generate a scatter column chart and perform statistical analysis. One-way analysis of variance (ANOVA) with Newman–Keuls multiple-comparison tests was performed with the significance level set to less than 0.01. Statistical analysis was performed to decide the sample size used in mouse infection by the Institute of Mathematics, University of Wurzburg under the allowance A2 55.5-2531.01-49/12. All mouse experiments were carried out with five female mice per treatment group. Mice in each experiment were age-matched and cage mates were randomly distributed into different treatment groups to avoid cage effects. Three mice were used for the gene expression experiment.

Isolation of human and mouse neutrophils. Human neutrophils were isolated as previously described using a density gradient method[40]. Briefly, heparinized venous blood was collected from healthy individuals and separated using a Ficoll gradient (Ficoll-plaque PLUS, 1.078 g ml^{-1}, GE Healthcare Life Science). The layers containing plasma and peripheral blood mononuclear cells were aspirated carefully, preserving the erythrocyte/granulocyte layer. Erythrocytes were aggregated by mixing with polyvinyl alcohol solution (1% polyvinyl alcohol in 0.85% saline), followed by incubation for 45 min at room temperature, leading to sedimentation. The supernatant was collected and residual erythrocytes were lysed with sterile water, followed by reconstitution of osmolarity with the addition of 5× Dulbecco's PBS. Finally, granulocytes were collected by centrifugation at 1,000 *g* for 5 min. The cell pellet was reconstituted in 1 × Hank's balanced salt solution (HBSS, Gibco). Neutrophil purity was determined by detecting surface expression of CD11b and CD66b antigens using flow cytometry (Accuri C6, BD Biosciences) (Supplementary Fig. 1a).

Mouse neutrophils were isolated from bone marrow as described previously[41]. Briefly, femur and tibia were extracted from euthanized mice. The epiphyses of the bone were removed to extract the bone marrow cells using a syringe. The cells were centrifuged at 427*g* for 7 min at 4 °C. The cells were further suspended in 20 ml of 0.2% NaCl for 20 s followed by the addition of 20 ml 1.6% NaCl to lyse the red blood cells. The bone marrow cells were further layered on Histopaque 1077 overlaid on Histopaque 1119. The gradient was further centrifuged at 872*g* for 30 min at room temperature. The cells collected at the interface were washed with PBS, and further resuspended in RPMI 1640 supplemented with 5% FBS. The cells were stained with Ly6G/CD11b antibody and analysed using flow cytometry to confirm the purity (Supplementary Fig. 4).

Neutrophil depletion. Neutrophils were depleted in C57BL/6 mice by a single intraperitoneal injection of 0.5 mg of anti-Ly6G clone 1A8 (BioXCell) per mouse. Control mice were injected with 0.5 mg of IgG2a (BioXCell). Circulating neutrophil depletion was confirmed by extracting 100 µl of venus blood and differential blood cell counts were assessed by FACS analyses (Supplementary Fig. 4). The mice were infected 6 h before injection with depleting antibody. The infected mice were euthanized 7 days post-infection, and the uterine horns were taken for analysis.

Neutrophil infection with *Chlamydia trachomatis*. Human/mouse neutrophils were suspended in HBSS media and infected with the indicated MOI of *Chlamydia*. Depending on the assay, the neutrophils were either allowed to adhere to tissue culture surface before infection by centrifugation at 500 *g* for 5 min or the cells were transferred into 1.5 ml microfuge tubes and infected with the indicated MOI of *Chlamydia*, followed by tumbling on a rotation wheel.

Copy-number determination of *Chlamydia* in neutrophils. A total of 1×10^6 neutrophils were infected with Ctr at a MOI 10. The cells were incubated for the required time points. The cells were washed and centrifuged to isolate DNA using DNAzol reagent. The genomic DNA was used to determine the copy number of bacteria per host cell. Human *cMyc* was used to normalize the host copy number using the primer: fwd, 5′-AGAGTTTCATCTGCGACCCG-3′ and rev, 5′-GATCCTGCAGGTACAAGATG-3′. The chlamydial *lytA* gene was amplified using the above-mentioned primer pair.

NET induction and quantification. Human neutrophils were suspended in HBSS media and seeded in a 96-well plate. Subsequently, the cells were infected with the indicated MOI of *Chlamydia* or treated with PMA. The cells were incubated at 37 °C in an incubator for 4 h. The quantification of NETs was performed as described in ref. [42]. Briefly, the supernatant was carefully removed and the cells were treated with micrococcal nuclease (500 mU ml^{-1}, Biolabs) for 15 min in the presence of $CaCl_2$ (1.5 mM). EDTA (5 mM) was added to inhibit nuclease activity. The amount of extracellular DNA in the supernatant of cells was then quantified using PicoGreen (Invitrogen) staining; the fluorescence was detected using a TECAN Infinite 200 plate reader. Each sample was processed in triplicate to avoid any bias in the reading.

Scanning electron microscopy and transmission electron microscopy. For scanning electron microscopy, the human neutrophils were grown on glass coverslips, and infected with wild-type/CPAF-deficient *Chlamydia* or treated with 50 ng ml^{-1} PMA on glass slide. The cells were fixed overnight with 6.25% glutaraldehyde in 50 mM phosphate buffer with pH 7.4. The cells were subsequently washed with Sörensen buffer (100 mM KH_2PO_4 and 100 mM Na_2HPO_4). The dehydration procedure was performed sequentially with 30%, 50%, 75%, 90% and 100% acetone for 5 min. Then, the cells were dried in a critical point dryer (BAL TEC, CPD 030) and coated with gold–palladium. The samples were analysed using a scanning electron microscope (JEOL JSM-7500F). Electron micrographs were processed using ImageJ (Fiji). For transmission electron microscopy, after infection, the cells were fixed with 2.5% glutaraldehyde (50 mM sodium cacodylate (pH 7.2), 50 mM KCl, 2.5 mM $MgCl_2$) at room temperature. The cells were incubated for 2 h at 4 °C with 2% OsO_4 buffered with 50 mM sodium cacodylate (pH 7.2), washed with distilled H_2O and incubated overnight at 4 °C with 0.5% uranyl acetate (in distilled H_2O). The cells were dehydrated, embedded in Epon812 and ultrathin-sectioned at 50 nm. Sections were stained with 2% uranyl acetate in ethanol followed by staining with lead citrate and analysed in a Zeiss EM10 microscope (Zeiss). Electron micrographs were processed using ImageJ (Fiji).

Infectivity assay. Human neutrophils were infected with wild-type or CPAF-deficient *Chlamydia* for 30 min or 24 h. The cells were then lysed using glass beads and different dilutions were used to infect freshly plated HeLa cells. After 36 h, the cells were lysed and western blot analysis was performed to detect cHSP60 as a marker for *Chlamydia* infection. β-Actin was used as a loading marker.

Western blot. Lysates for western blot analysis were prepared by directly lysing cells in Laemmli buffer (62.5 mM Tris, pH 6.8, 2% SDS, 20% glycerol and 5% β-mercaptoethanol). Western blot analysis was performed as described in ref. [43]. The antibody against FPR2 was purchased from Abcam. The pan-PKC, p-pan-PKC, ERK, pERK, protein kinase B (AKT) and pAKT antibodies were obtained from Cell Signaling. The mouse anti-CPAF-c antibody was a generous gift from G. Zhong, University of Texas Health Science Center at San Antonio. Chlamydial HSP60 (cHSP60) antibody was purchased from Santa Cruz and β-actin antibody from Sigma.

Calcium mobilization in PMNs and HL60. Calcium fluxes were analysed by stimulating cells loaded with Fluo-3-AM (Molecular Probes) and monitoring fluorescence using a flow cytometer (Accuri C6, BD) with a FL-1 filter (excitation 488 nm/emission 530 ± 15 nm band-pass) as recently described[44]. Agonists were used at the following final concentrations: 1 nM fMLP (Sigma-Aldrich), 62.5 nM MMK1 (Alomone Labs). HL60 cells were stimulated with fMLP and MMK1 using final peptide concentrations of 20 nM and 10 nM, respectively. Measurements were performed for 30 s and the calcium flux was expressed as relative fluorescence normalized to buffer controls.

Measuring FPR1/FPR2 or CD11b on cell surface. Human neutrophils were isolated and infected with respective bacteria for the specified period of time. Subsequently, the cells were centrifuged at 500 *g* for 5 min and resuspended in the blocking buffer (HBSS with 2% BSA). The cells were then stained with fluorescein isothiocyanate (FITC)-coupled anti-human FPR1 and phycoerythrin-conjugated anti-human FPR2 (BD Biosciences) for 30 min at 4 °C. CD11b staining was performed using a human CD11b antibody conjugated with PE (Miltenyi Biotec). The cells were then washed with blocking buffer and fluorescence levels were analysed with a flow cytometer (Accuri C6, BD Biosciences) using the FL-1 filter (excitation 488 nm/emission 530 ± 15 nm band-pass) and the FL-2 filter (excitation 488 nm/emission 585 ± 40 nm band-pass), which determined the expression on the cell surface. Measurements of 10,000 events were performed and were expressed as relative fluorescence corrected for isotype controls.

ELISA to detect FPR2. Human neutrophils were plated in a white 96-well plate. The cells were infected with CtrWT or RST17(CPAF$^-$) or the neutrophils were treated with active/inactive recombinant CPAF. After 4 h of incubation, the supernatant of the cells was collected and centrifuged at high speed to remove cell debris. The supernatant was used to detect levels of FPR2 using ELISA kit (Biomatik) according to the manufacturer's instructions. The relative fluorescence from an uninfected sample was used for normalization.

Luminol assay. ROS production in neutrophils after *Chlamydia* infection was measured using luminol bioluminescence as previously described[45]. The cells

(5×10^4 per well) were seeded in a white 96-well plate (Nunclon). The cells were either left uninfected or infected with CtrWT or RST17(CPAF$^-$) at a MOI of 10 for 30 min. The cells were further challenged with PMA (5 ng ml^{-1}). For the assay, luminol (Sigma-Aldrich) was added at a final concentration of 50 µM and the luminescence was measured using a TECAN Infinite 200 plate reader every minute for 30 min.

Recombinant CPAF protein preparation. Constructs to generate recombinant CPAF were cloned into the pETM11 vector. The expression construct did not contain the first amino-terminal 21 amino acids and thus represented the coding sequence of the active CPAF. For recombinant protein expression, recombinant *Escherichia coli* BL21 pRARE were grown overnight at 15 °C in the presence of 0.5 mM isopropyl-β-D-thiogalactoside. Bacterial cells were collected by centrifugation, and lysed in 50 mM Hepes pH 7.5 containing 100 mM NaCl, 5 mM β-mercaptoethanol, 0.5 mM phenylmethylsulfonyl fluoride and protease inhibitors. After removal of cell debris, soluble recombinant proteins were eluted using glutathione beads (Thermo Fischer). Recombinant proteins were digested with TEV protease, eluted and further purified by gel-filtration chromatography using Supadex 200 columns and Sepharose 6 columns.

Synthetic peptides. Anti-CPAF (SLFYSPMVPHFWAELRNHYATSGLK) and scrambled peptide (NFALSHFRLPLSTYKEMPYVSHWAG)[26], which lack arginine tails, were synthesized by Pepmic and Co, China. The FPR2/ALX-specific control ligand MMK1 (LESIFRSLLFRVM-NH_2)[46] was obtained from Sigma, and the FPR2/ALX inhibitor WRW4 (WRWWWW-NH_2)[47,48] from Abcam. The FPR1-specific ligand fMLP was purchased from Sigma and its antagonist Boc-MLF from Tocris Biosciences.

Degranulation assay. CD35 (complement receptor 1) and CD66b (CAECAM-8) were examined as markers for neutrophil degranulation and secretory vesicle/granule mobilization, respectively. Human neutrophils were isolated and infected with the respective MOI of wild-type or CPAF-deficient *Chlamydia* for 1 h. fMLP (1 µM) was used as a positive control for stimulation. The cells were then stained with phycoerythrin-conjugated human CD35 (BD Biosciences) or phycoerythrin-conjugated CD66b (BD Biosciences) as instructed by the manufacturer. The stained cells were analysed via FACS (Accuri C6, BD Biosciences). A total of 10,000 events were collected for each sample. Mean channel fluorescence was measured from the neutrophil-gated cells. All relative fluorescence data were expressed as a percentage of fMLP to adjust for physiological sample-to-sample variation. Percentage stimulation was calculated by dividing each sample mean fluorescence value by the mean fluorescence value of fMLP and multiplying by 100.

Real-time PCR. RNA was isolated from uninfected or wild-type/CPAF-deficient *Chlamydia*-infected neutrophils using the RNA easy kit (Qiagen, Germany). RNA was reverse-transcribed using a Revert Aid First Strand synthesis Kit (Fermentas) according to the manufacturer's instructions and diluted 1:10 with RNase-free water. Quantitative RT-PCR was performed as previously described[49]. Briefly, quantitative RT-PCR reactions were prepared with Quanta SYBR (Quanta Bio) and PCR was performed on a Step One Plus device (Applied Biosystems). The data were analysed using the ΔΔCt method, Step One Plus software package (Applied Biosystems) and Excel (Microsoft). The endogenous control was GAPDH. Primers were designed by qPrimer Depot. Primers for human GAPDH: fwd, 5′-GAAGGTGAAGGTCGGAGTCAAC-3′ and rev, 5′-GAAGATGGTGATGGGATTTC-3′; human FPR2: fwd, 5′-TCTTGCTCTAGTCCTTACCTTGC-3′ and rev, 5′-AATGACAAACCGGATAATCCCTC-3′; human IL-8: fwd, 5′-ATGACTTCCAAGCTGGCCGTGGCT-3′ and rev, 5′-TCTCAGCCCTCTTCAAAAACTTCT-3′; mouse FPR2: fwd, 5′-ATCCAGAACGATGTAGCCAGCA-3′ and rev, 5′-AGACCTCAGCTGGTTGTGCAG-3′; mouse GAPDH: fwd, 5′-ACCACAGTCCATGCCATCAC-3′ and rev, 5′-CACCACCCTGTTGCTGTAGCC-3′.

Chemotaxis. Migration of neutrophils towards wild-type *Chlamydia* or synthetic peptides was determined by using neutrophils labelled with the fluorescent dye CFSE (5-(and-6)-carboxyfluorescein diacetate, succinimidyl ester, Invitrogen), in a 3-µm-pore-size polycarbonate Trans-well filter (Sarstedt), as described earlier[50]. Synthetic chemoattractant was used at concentrations in the linear range of the dose–response curves. Neutrophil migration from the upper to the lower Trans-well chamber was observed only when the chemoattractant (MMK1) was added to the lower chamber. The relative fluorescence measured was corrected for the buffer control (only buffer added to the lower compartment).

Statistical methods. In all experiments, two or three technical replicates were used and the *n* number refers to the number of independent experiments performed. For human blood, random healthy volunteers were chosen as donors. The data are presented as box-and-whisker plots with all box elements (median, upper and lower quartiles, range) or as mean and s.e.m. Statistical analyses were performed with the Prism 4.0 and 7.2 package (GraphPad Software) and R statistical package.

The power of tests and *n* required for statistical significance were calculated by using η^2 (eta squared) in the 'lsr' package and the 'pwr' package in R (https://github.com/heliosdrm/pwr).

For one and two-way ANOVA, assumption of normality was performed by fitting data to a linear model. Normality was determined by *F*-statistic, correlation coefficient (R^2) and normal quantile–quantile plots.

Data sets that violated the assumption of normality (that is, non-parametric data) were analysed with the Kruskal–Wallis rank sum test followed by Dunn's test for multiple comparisons (one-factorial) and the Durbin and Conover test for a two-way balanced incomplete block design with a pairwise post hoc test (two-factorial).

No data were excluded from analyses and the investigators were not blinded during group allocation.

Reporting Summary. Further information on experimental design is available in the Nature Research Reporting Summary linked to this article.

Data availability. The data that support the findings of this study are available from the corresponding author upon request.

Received: 24 April 2017; Accepted: 18 May 2018;
Published online: 25 June 2018

References

1. Brinkmann, V. et al. Neutrophil extracellular traps kill bacteria. *Science* **303**, 1532–1535 (2004).
2. Murphy, P. M. et al. A structural homologue of the N-formyl peptide receptor. Characterization and chromosome mapping of a peptide chemoattractant receptor family. *J. Biol. Chem.* **267**, 7637–7643 (1992).
3. Kretschmer, D. et al. Human formyl peptide receptor 2 senses highly pathogenic *Staphylococcus aureus*. *Cell Host Microbe* **7**, 463–473 (2010).
4. von Kockritz-Blickwede, M., Blodkamp, S. & Nizet, V. Interaction of bacterial exotoxins with neutrophil extracellular traps: impact for the infected host. *Front. Microbiol.* **7,** 402 (2016).
5. Paavonen, J. & Eggert-Kruse, W. *Chlamydia trachomatis*: impact on human reproduction. *Hum. Reprod. Update* **5**, 433–447 (1999).
6. Fleming, D. T. & Wasserheit, J. N. From epidemiological synergy to public health policy and practice: the contribution of other sexually transmitted diseases to sexual transmission of HIV infection. *Sex. Transm. Infect.* **75**, 3–17 (1999).
7. Vonck, R. A., Darville, T., O'Connell, C. M. & Jerse, A. E. Chlamydial infection increases gonococcal colonization in a novel murine coinfection model. *Infect. Immun.* **79**, 1566–1577 (2011).
8. Herweg, J. A. & Rudel, T. Interaction of Chlamydiae with human macrophages. *FEBS J.* **283**, 608–618 (2016).
9. Fischer, A. & Rudel, T. Subversion of cell-autonomous host defense by *Chlamydia* infection. *Curr. Top. Microbiol. Immunol.* https://doi.org/10.1007/82_2016_13 (2016).
10. Dicker, L. W., Mosure, D. J., Berman, S. M. & Levine, W. C. Gonorrhea prevalence and coinfection with chlamydia in women in the United States, 2000. *Sex. Transm. Dis.* **30**, 472–476 (2003).
11. Criss, A. K. & Seifert, H. S. A bacterial siren song: intimate interactions between *Neisseria* and neutrophils. *Nat. Rev. Microbiol.* **10**, 178–190 (2012).
12. Huang, Z. et al. Structural basis for activation and inhibition of the secreted chlamydia protease CPAF. *Cell Host Microbe* **4,** 529–542 2008).
13. Saka, H. A. et al. Quantitative proteomics reveals metabolic and pathogenic properties of *Chlamydia trachomatis* developmental forms. *Mol. Microbiol.* **82**, 1185–1203 (2011).
14. Chen, D. et al. Autoprocessing and self-activation of the secreted protease CPAF in *Chlamydia*-infected cells. *Microb. Pathog.* **49**, 164–173 (2010).
15. Yang, Z., Tang, L., Zhou, Z., & Zhong, G. Autoprocessing and self-activation of the secreted protease CPAF in *Chlamydia*-infected cells. *Microb. Pathog.* **49**, 164–173 (2010).
16. Tang, L. et al. *Chlamydia*-secreted protease CPAF degrades host antimicrobial peptides. *Microbes Infect.* **17**, 402–408 (2015).
17. Yang, Z. et al. The *Chlamydia*-secreted protease CPAF promotes chlamydial survival in the mouse lower genital tract. *Infect. Immun.* **84**, 2697–2702 (2016).
18. Snavely, E. A. et al. Reassessing the role of the secreted protease CPAF in *Chlamydia trachomatis* infection through genetic approaches. *Pathog. Dis.* **71**, 336–351 (2014).
19. Frazer, L. C., O'Connell, C. M., Andrews, C. W. Jr, Zurenski, M. A. & Darville, T. Enhanced neutrophil longevity and recruitment contribute to the severity of oviduct pathology during *Chlamydia muridarum* infection. *Infect. Immun.* **79**, 4029–4041 (2011).
20. Reeves, E. P. et al. Killing activity of neutrophils is mediated through activation of proteases by K^+ flux. *Nature* **416**, 291–297 (2002).

21. Daley, J. M., Thomay, A. A., Connolly, M. D., Reichner, J. S. & Albina, J. E. Use of Ly6G-specific monoclonal antibody to deplete neutrophils in mice. *J. Leukoc. Biol.* **83**, 64–70 (2008).
22. Brinkmann, V. & Zychlinsky, A. Neutrophil extracellular traps: is immunity the second function of chromatin? *J. Cell Biol.* **198,** 773–783 2012).
23. Pettit, E. J. & Hallett, M. B. Two distinct Ca^{2+} storage and release sites in human neutrophils. *J. Leukoc. Biol.* **63**, 225–232 (1998).
24. Bednar, M. M., Jorgensen, I., Valdivia, R. H. & McCafferty, D. G. *Chlamydia* protease-like activity factor (CPAF): characterization of proteolysis activity in vitro and development of a nanomolar affinity CPAF zymogen-derived inhibitor. *Biochemistry* **50**, 7441–7443 (2011).
25. Bae, Y. S. et al. Identification of peptides that antagonize formyl peptide receptor-like 1-mediated signaling. *J. Immunol.* **173**, 607–614 (2004).
26. Jorgensen, I. et al. The *Chlamydia* protease CPAF regulates host and bacterial proteins to maintain pathogen vacuole integrity and promote virulence. *Cell Host Microbe* **10**, 21–32 (2011).
27. Gray, R. D. et al. Activation of conventional protein kinase C (PKC) is critical in the generation of human neutrophil extracellular traps. *J. Inflamm.* **10**, 12 (2013).
28. Hakkim, A. et al. Activation of the Raf–MEK–-ERK pathway is required for neutrophil extracellular trap formation. *Nat. Chem. Biol.* **7**, 75–77 (2011).
29. von Kockritz-Blickwede, M. & Nizet, V. Innate immunity turned inside-out: antimicrobial defense by phagocyte extracellular traps. *J. Mol. Med* **87**, 775–783 (2009).
30. Buchholz, K. R. & Stephens, R. S. The extracellular signal-regulated kinase/mitogen-activated protein kinase pathway induces the inflammatory factor interleukin-8 following *Chlamydia trachomatis* infection. *Infect. Immun.* **75**, 5924–5929 (2007).
31. Darville, T. & Hiltke, T. J. Pathogenesis of genital tract disease due to *Chlamydia trachomatis*. *J. Infect. Dis.* **201**, S114–S125 (2010).
32. Bai, H. et al. Intranasal inoculation of *Chlamydia trachomatis* mouse pneumonitis agent induces significant neutrophil infiltration which is not efficient in controlling the infection in mice. *Immunology* **114**, 246–254 (2005).
33. Barteneva, N., Theodor, I., Peterson, E. M. & de la Maza, L. M. Role of neutrophils in controlling early stages of a *Chlamydia trachomatis* infection. *Infect. Immun.* **64**, 4830–4833 (1996).
34. Tan, M. & Sutterlin, C. The *Chlamydia* protease CPAF: caution, precautions and function. *Pathog. Dis.* **72**, 7–9 (2014).
35. Prince, L. R., Whyte, M. K., Sabroe, I., & Parker, L. C. The role of TLRs in neutrophil activation. *Curr. Opin. Pharmacol.* **11,** 397–403 2011).
36. Al-Younes, H. M., Rudel, T., Brinkmann, V., Szczepek, A. J. & Meyer, T. F. Low iron availability modulates the course of *Chlamydia pneumoniae* infection. *Cell. Microbiol.* **3**, 427–437 (2001).
37. Christophe, T. et al. The synthetic peptide Trp-Lys-Tyr-Met-Val-Met-NH2 specifically activates neutrophils through FPRL1/lipoxin A4 receptors and is an agonist for the orphan monocyte-expressed chemoattractant receptor FPRL2. *J. Biol. Chem.* **276**, 21585–21593 (2001).
38. Dahlgren, C. et al. The synthetic chemoattractant Trp-Lys-Tyr-Met-Val-DMet activates neutrophils preferentially through the lipoxin A(4) receptor. *Blood* **95**, 1810–1818 (2000).
39. Chen, K. et al. A critical role for the g protein-coupled receptor mFPR2 in airway inflammation and immune responses. *J. Immunol.* **184**, 3331–3335 (2010).
40. Hattar, K. et al. Subthreshold concentrations of anti-proteinase 3 antibodies (c-ANCA) specifically prime human neutrophils for fMLP-induced leukotriene synthesis and chemotaxis. *J. Leukoc. Biol.* **69**, 89–97 (2001).
41. Swamydas, M., Luo, Y., Dorf, M. E. & Lionakis, M. S. Isolation of mouse neutrophils. *Curr. Protoc. Immunol.* **110**, 3.20.21–3.20.15 (2015).
42. Gonzalez, A. S., Bardoel, B. W., Harbort, C. J. & Zychlinsky, A. Induction and quantification of neutrophil extracellular traps. *Methods Mol. Biol.* **1124**, 307–318 (2014).
43. Karunakaran, K., Mehlitz, A. & Rudel, T. Evolutionary conservation of infection-induced cell death inhibition among Chlamydiales. *PLoS ONE* **6**, e22528 (2011).
44. de Haas, C. J. et al. Chemotaxis inhibitory protein of *Staphylococcus aureus*, a bacterial antiinflammatory agent. *J. Exp. Med.* **199**, 687–695 (2004).
45. Yamazaki, T., Kawai, C., Yamauchi, A. & Kuribayashi, F. A highly sensitive chemiluminescence assay for superoxide detection and chronic granulomatous disease diagnosis. *Trop. Med. Health* **39**, 41–45 (2011).
46. Fu, H. et al. Ligand recognition and activation of formyl peptide receptors in neutrophils. *J. Leukoc. Biol.* **79**, 247–256 (2006).
47. Karlsson, J., Fu, H., Boulay, F., Bylund, J. & Dahlgren, C. The peptide Trp-Lys-Tyr-Met-Val-D-Met activates neutrophils through the formyl peptide receptor only when signaling through the formylpeptide receptor like 1 is blocked. A receptor switch with implications for signal transduction studies with inhibitors and receptor antagonists. *Biochem. Pharmacol.* **71**, 1488–1496 (2006).
48. Onnheim, K., Bylund, J., Boulay, F., Dahlgren, C. & Forsman, H. Tumour necrosis factor (TNF)-α primes murine neutrophils when triggered via formyl peptide receptor-related sequence 2, the murine orthologue of human formyl peptide receptor-like 1, through a process involving the type I TNF receptor and subcellular granule mobilization. *Immunology* **125**, 591–600 (2008).
49. Karunakaran, K., Subbarayal, P., Vollmuth, N. & Rudel, T. *Chlamydia*-infected cells shed Gp96 to prevent chlamydial re-infection. *Mol. Microbiol* **98**, 694–711 (2015).
50. Durr, M. C. et al. Neutrophil chemotaxis by pathogen-associated molecular patterns - formylated peptides are crucial but not the sole neutrophil attractants produced by *Staphylococcus aureus*. *Cell. Microbiol.* **8**, 207–217 (2006).

Acknowledgements

We thank D. Kretschmer and A. Peschel (Univeristy of Tübingen) for providing the HL60 cell lines and HL60 expressing FPR1 and FPR2. We thank R. Valdivia and E. Snavely (Duke University) for the CPAF-deficient and complemented strain of *Chlamydia*, G. Zhong (University of Texas) for the CPAF antibody and P. Lüningschrör (University of Würzburg) for the mouse synectin plasmid. We are grateful to O. Söhnlein (LMU Munich) for providing the FPR2-KO mice. C. Gehrig and D. Bunsen supported the scanning and transmission electron microscopy analyses. We acknowledge J. Sühlfleisch, N. Vollmuth and H. Czotscher for technical assistance. We thank S. Gorski, R. Sivadasan and A. Demuth for critically reading the manuscript. K.R. was supported by funds of the Frauenbüro, University of Würzburg. S.D. was funded by the Career Development Fellowship from the Graduate School of Life Sciences, University of Würzburg. This work was supported by Deutsche Forschungsgemeinschaft - GRK 2157 to T.R.

Author contributions

K.R., S.D. and T.R. conceived and designed the study. K.R. performed all of the experiments, except for the experiments shown in Figs. 3a,b and 4f, which were carried out by S.D. Data analysis was performed by K.R and S.D. B.K.P. provided active and inactive recombinant CPAF. K.R. and T.R. wrote the manuscript.

Competing interests

The authors declare no competing interests.

Additional information

Supplementary information is available for this paper at https://doi.org/10.1038/s41564-018-0182-y.

Reprints and permissions information is available at www.nature.com/reprints.

Correspondence and requests for materials should be addressed to T.R.

Publisher's note: Springer Nature remains neutral with regard to jurisdictional claims in published maps and institutional affiliations.

nature research

Corresponding author(s): Prof. Dr. Thomas Rudel

Life Sciences Reporting Summary

Nature Research wishes to improve the reproducibility of the work that we publish. This form is intended for publication with all accepted life science papers and provides structure for consistency and transparency in reporting. Every life science submission will use this form; some list items might not apply to an individual manuscript, but all fields must be completed for clarity.

For further information on the points included in this form, see Reporting Life Sciences Research. For further information on Nature Research policies, including our data availability policy, see Authors & Referees and the Editorial Policy Checklist.

Please do not complete any field with "not applicable" or n/a. Refer to the help text for what text to use if an item is not relevant to your study.
For final submission: please carefully check your responses for accuracy; you will not be able to make changes later.

Experimental design

1. Sample size

   Describe how sample size was determined.

   To determine the number of replicates (sample size) required of each statistical test to be powerful enough test the hypothesis, we used the 'pwr' package in R. The statistics on the mouse infection sample size was done by the Institute of Mathematik, University of Wurzburg under the allowance A2 55.5-2531.01-49/12.

2. Data exclusions

   Describe any data exclusions.

   No data was excluded.

3. Replication

   Describe the measures taken to verify the reproducibility of the experimental findings.

   For neutrophil studies, we used different healthy donors to rule out donor effects and to check reproducibility. We applied multiple testing wherever we performed statistical test to describe the robustness. All attempts at replication were successful.

4. Randomization

   Describe how samples/organisms/participants were allocated into experimental groups.

   Our study involved biological assays where groups were predetermined according to conditions. Hosts (PMNs, human cell lines, mice) were randomly assigned to each condition unless different host types (knock out organisms were used), where host groups were also a predetermined condition.

5. Blinding

   Describe whether the investigators were blinded to group allocation during data collection and/or analysis.

   The experiments were blinded and animals were age-matched and cage mates were randomly distributed into different treatment groups to avoid cage effects.

Note: all in vivo studies must report how sample size was determined and whether blinding and randomization were used.

6. Statistical parameters

For all figures and tables that use statistical methods, confirm that the following items are present in relevant figure legends (or in the Methods section if additional space is needed).

n/a	Confirmed
☐	☒ The exact sample size (*n*) for each experimental group/condition, given as a discrete number and unit of measurement (animals, litters, cultures, etc.)
☐	☒ A description of how samples were collected, noting whether measurements were taken from distinct samples or whether the same sample was measured repeatedly
☐	☒ A statement indicating how many times each experiment was replicated
☐	☒ The statistical test(s) used and whether they are one- or two-sided *Only common tests should be described solely by name; describe more complex techniques in the Methods section.*
☐	☒ A description of any assumptions or corrections, such as an adjustment for multiple comparisons
☐	☒ Test values indicating whether an effect is present *Provide confidence intervals or give results of significance tests (e.g. P values) as exact values whenever appropriate and with effect sizes noted.*
☐	☒ A clear description of statistics including central tendency (e.g. median, mean) and variation (e.g. standard deviation, interquartile range)
☐	☒ Clearly defined error bars in all relevant figure captions (with explicit mention of central tendency and variation)

See the web collection on statistics for biologists for further resources and guidance.

Software

Policy information about availability of computer code

7. Software

Describe the software used to analyze the data in this study.	Prism (4.0 and 7.2 Graph pad software) and R Statistical software were use for statistical analysis. Step one soft ware was used for analyzing quantitative PCR and LAS-AF software, Image J and Gimp2 was used for analyzing the immune stained images and Western blot images.

For manuscripts utilizing custom algorithms or software that are central to the paper but not yet described in the published literature, software must be made available to editors and reviewers upon request. We strongly encourage code deposition in a community repository (e.g. GitHub). *Nature Methods* guidance for providing algorithms and software for publication provides further information on this topic.

Materials and reagents

Policy information about availability of materials

8. Materials availability

Indicate whether there are restrictions on availability of unique materials or if these materials are only available for distribution by a third party.	All unique materials are available from the authors

9. Antibodies

Describe the antibodies used and how they were validated for use in the system under study (i.e. assay and species).

1. c HSP60- Santa cruz, Catalog Number- sc-57840, Clone name- A57-B9, Lot Number- D2216. Dilution used- 1:1000 used for Western blots and 1:500 for immuno staining, Validation statement given by the producer.
2. ß Actin- Sigma, Catalog Number- A5441, Clone name- AC-15, Lot Number- 026M4780V. Dilution used 1:10000 used for Western blots, Validation statement given by the producer.
3. Ngo- US biologicals, Catalog Number- N0600-02, Clone name-Pab, Lot Number L14031112C15032655. Dilution used 1:300 used for Immuno staining, Validation statement given by the producer.
4.pPKC- Cell Signaling, Catalog Number- cs-9379, Clone Name-not provided, Lot Number-2. Dilution used - 1.1000 for Western blots. Validation statement given by the producer.
5. TPKC- Merck Millipore, Catalog Number279485, Clone Name-M110, Lot Number-279485. Dilution used - 1.1000 for Western blots. Validation statement given by the producer.
6. CD11b- Milteny Biotech, Catalog Number-130-091-240, clone: M1/70.15.11.5, Lot number-5161020426. Dilution used 1:200 for FACS, Validation statement given by the producer.
7. FPR1- R and D, Catalog Number-FAB3744P, Clone name- not provided, Lot Number-AAGG0215031. Dilution used 1:400 for FACS. Validation statement given by the producer.
8. FPR2- R and D, Catalog Number-FAB3479P, Clone name- not provided, Lot Number-LZV0215101. Dilution used 1:400 for FACS. Validation statement given by the producer.
9. His tag- Acris, Catalog Number- GTX18184, Clone name-His.H8, Lot Number-R33257. Dilution used 1:1000 for Western blot. Validation statement given by the producer.
10. pAkt-Cell Signaling, Catalog Number-cs-9275, Clone name-not provided, Lot Number-21. Dilution used 1:1000 for Western blot. Validation statement given by the producer.
11. T-Akt-Cell Signaling, Catalog Number-cs-4691, Clone name-C67E7, Lot Number-3. Dilution used 1:1000 for Western blot. Validation statement given by the producer.
12.pERK-Cell Signaling, Catalog Number-cs-9106, Clone name-E10, Lot Number-43. Dilution used 1:1000 for Western blot. Validation statement given by the producer.
13. T-ERK-Cell Signaling, Catalog Number-cs-9108), Clone name-not provided, Lot Number-6. Dilution used 1:1000 for Western blot. Validation statement given by the producer.
14.CD35-BioLengend, Catalog Number-333405, Clone name-E11, Lot Number-B217714. Dilution used 1:200 for FACS. Validation statement given by the producer.
15. CD66b- BD Pharmingen, Catalog Number-561650, Clone name-G10F5, Lot Number-5156843. Dilution used 1:400 for FACS. Validation statement given by the producer.
16. Ly6G-BioXCell, Catalog Number-BP0075-1), Clone name -1A8, Lot Number-626717M2B. 0.5 mg In vivo injection per mouse. Validation statement given by the producer.
17. IgG2a-BioXCell, Catalog Number-BE0085, Clone name-C1.18.4, Lot Number-655217M2. 0.5 mg In vivo injection per mouse. Validation statement given by the producer.
18. GP91 phox-Santa cruz, Catalog Number-sc-5827, Clone name-G1, Lot Number-C0529. Dilution used 1:500 for Western blot. Validation statement given by the producer.
19. DUOX-Santa cruz, Catalog Number-sc-98898, Clone name-H-9, Lot Number-C0209. Dilution used 1:500 for Western blot. Validation statement given by the producer
20. GFP-Santa cruz, Catalog Number-sc-9996, Clone name-B-2, Lot Number-K1815. Dilution used 1:500 for Western blot. Validation statement given by the producer
21. Vimentin-Santa cruz, Catalog Number-sc-73259, Clone name-C20, Lot Number- H2007. Dilution used 1:500 for Western blot. Validation statement given by the producer
22. CD63-BioLengend, Catalog Number-353003, Clone name- H5C6, Lot Number- B184017. Dilution used 1:500 for Western blot. Validation statement given by the producer
23. CPAF- serum obtained from Dr. Guangming Zhong, University of Texas Health Science Center at San Antonio- Western blot and Immunostaining. Clone name -100a. Dilution used 1:500 for Western blot. Validation shown in Dong et al 2004.
24. CD11b- BD Bioscience, Catalog Number- 555388, Clone name-ICRF44, Lot Number-6133542 - Dilution used 1:500 for Western blot. Validation statement given by the producer
25. GSK3-Cell signaling, Catalog Number-9832, Clone name-3D10, Lot Number- 3. Dilution used 1:500 for Western blot. Validation statement given by the producer

10. Eukaryotic cell lines

a. State the source of each eukaryotic cell line used.

1. HeLa229 (ATCC CCL-2.1).
2. HL60 (ATCC® CCL-240™) were obtained from Dorothee Kretschmer and Andreas Peschel (Universität Tübingen, Germany).

b. Describe the method of cell line authentication used.

Cell lines were authenticated by ATCC: ATCC uses morphology, karyotyping, and PCR based approaches to confirm the identity of human cell lines and to rule out both intra- and interspecies contamination. These include an assay to detect species specific variants of the cytochrome C oxidase I gene (COI analysis) to rule out inter-species contamination and short tandem repeat (STR) profiling to distinguish between individual human cell lines and rule out intra-species contamination.

c. Report whether the cell lines were tested for mycoplasma contamination.

All the cells were regularly checked for Mycoplasma contamination and was tested negative.

d. If any of the cell lines used are listed in the database of commonly misidentified cell lines maintained by ICLAC, provide a scientific rationale for their use.

No commonly misidentified cell lines were used.

Animals and human research participants

Policy information about studies involving animals; when reporting animal research, follow the ARRIVE guidelines

11. Description of research animals

Provide all relevant details on animals and/or animal-derived materials used in the study.

All animal experiments were performed in accordance with protocols approved by animal care and experimentation of German Animal Protection Law approved under the Animal (Scientific Procedures) Act 1986 (project licence 55.2-2531.01-49/12). C57/BL6 and FPR2 KO female mouse were used in the study. The mice used for infection studies were female and were more than 8 weeks old. Statistical analysis was performed by the Department of Mathematik, University of Wuerzburg, to decide the sample size used in mouse infection. All mouse experiments were carried out with 5 female mice per treatment group. Mice in each experiment were age-matched and cage mates were randomly distributed into different treatment groups to avoid cage effects.

Policy information about studies involving human research participants

12. Description of human research participants

Describe the covariate-relevant population characteristics of the human research participants.

Blood was collected from random healthy donors.

Terms and Conditions

Springer Nature journal content, brought to you courtesy of Springer Nature Customer Service Center GmbH (“Springer Nature”).
Springer Nature supports a reasonable amount of sharing of research papers by authors, subscribers and authorised users (“Users”), for small-scale personal, non-commercial use provided that all copyright, trade and service marks and other proprietary notices are maintained. By accessing, sharing, receiving or otherwise using the Springer Nature journal content you agree to these terms of use (“Terms”). For these purposes, Springer Nature considers academic use (by researchers and students) to be non-commercial.
These Terms are supplementary and will apply in addition to any applicable website terms and conditions, a relevant site licence or a personal subscription. These Terms will prevail over any conflict or ambiguity with regards to the relevant terms, a site licence or a personal subscription (to the extent of the conflict or ambiguity only). For Creative Commons-licensed articles, the terms of the Creative Commons license used will apply.
We collect and use personal data to provide access to the Springer Nature journal content. We may also use these personal data internally within ResearchGate and Springer Nature and as agreed share it, in an anonymised way, for purposes of tracking, analysis and reporting. We will not otherwise disclose your personal data outside the ResearchGate or the Springer Nature group of companies unless we have your permission as detailed in the Privacy Policy.
While Users may use the Springer Nature journal content for small scale, personal non-commercial use, it is important to note that Users may not:

1. use such content for the purpose of providing other users with access on a regular or large scale basis or as a means to circumvent access control;
2. use such content where to do so would be considered a criminal or statutory offence in any jurisdiction, or gives rise to civil liability, or is otherwise unlawful;
3. falsely or misleadingly imply or suggest endorsement, approval , sponsorship, or association unless explicitly agreed to by Springer Nature in writing;
4. use bots or other automated methods to access the content or redirect messages
5. override any security feature or exclusionary protocol; or
6. share the content in order to create substitute for Springer Nature products or services or a systematic database of Springer Nature journal content.

In line with the restriction against commercial use, Springer Nature does not permit the creation of a product or service that creates revenue, royalties, rent or income from our content or its inclusion as part of a paid for service or for other commercial gain. Springer Nature journal content cannot be used for inter-library loans and librarians may not upload Springer Nature journal content on a large scale into their, or any other, institutional repository.
These terms of use are reviewed regularly and may be amended at any time. Springer Nature is not obligated to publish any information or content on this website and may remove it or features or functionality at our sole discretion, at any time with or without notice. Springer Nature may revoke this licence to you at any time and remove access to any copies of the Springer Nature journal content which have been saved.
To the fullest extent permitted by law, Springer Nature makes no warranties, representations or guarantees to Users, either express or implied with respect to the Springer nature journal content and all parties disclaim and waive any implied warranties or warranties imposed by law, including merchantability or fitness for any particular purpose.
Please note that these rights do not automatically extend to content, data or other material published by Springer Nature that may be licensed from third parties.
If you would like to use or distribute our Springer Nature journal content to a wider audience or on a regular basis or in any other manner not expressly permitted by these Terms, please contact Springer Nature at

onlineservice@springernature.com